Status and recent developments of the QUAX haloscope at Legnaro National Laboratories

Raffaele Di Vora

On behalf of the LNL section of the QUAX Collaboration

R. Di Vora, A. Lombardi, A. Ortolan, A. Gardikiotis, R. Pengo, and G. Ruoso (INFN-LNL)
C. Braggio (Unipd)
G. Carugno and L. Taffarello (INFN-Pd)

July 7, 2023

Istituto Nazionale di Fisica Nucleare
LABORATORI NAZIONALI DI LEGNARO

Outline I

- Introduction
  - Brief history of the QUAX-LNL experiment
- The Haloscope: a resonant DM axion detector
  - Expected axion signal
  - Noise background estimation
- Experimental setup
  - 8T Magnet
  - The high-Q dielectric cavity
  - Electronics setup
  - TWPA amplifier
- Auxiliary measurements and data acquisition routine
  - Calibration procedure
  - Data-taking procedure
- The QUAX-aγ 2022 measurement run

Outline II

- Run parameters overview
- Raw data processing
- Data analysis: Axion detection procedure
- Data analysis: upper limit on axion-photon coupling
- Run analysis results

- Cavity developments
  - TM_{010} tunable clamshell cavity
  - TM_{010} polygonal coaxial cavity

- Summary

- Future perspectives

- Backup slides

Brief history of the QUAX-LNL experiment

- 2015-2020: operation as pathfinder for ferromagnetic haloscope design; many technical challenges solved but sensitivity still low compared to expected signal
- Due to this, low interest in trying to scan in this mode → focus shifts to operation as demonstrator for haloscopes targeting high frequency regimes (10 GHz+)
- 2019: operation in traditional axion-photon haloscope mode starts, first run using superconductive TM_{010} Nb-Ti cavity, 2 T magnet and cryo HEMT amplifier operated at 4 K
- 2020: major upgrade in setup: dilution fridge implemented, bringing temperature down to ∼200 mK, 8 T magnet and JPA for total noise temperature of 1 K using Cu TM_{010} cavity
- 2021: implementation of high Q (10^7) dielectric cavity, but: frequency outside JPA range → low sensitivity first run using cryo HEMT and outside del fridge, $T_{sys} = 17$ K
- Now: first run using TWPA and dielectric cavity, high Q cavity and 8 T field

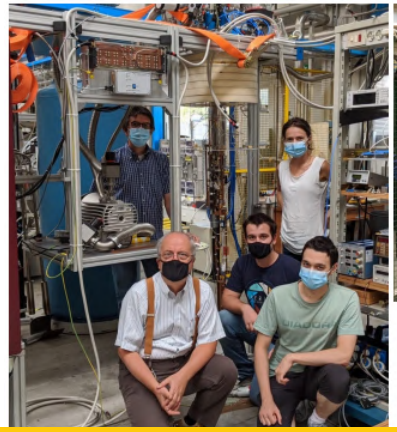

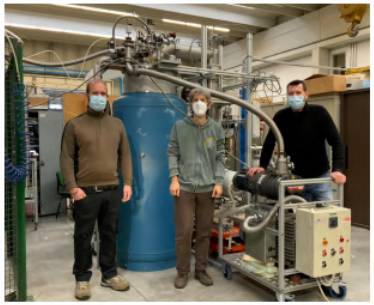

Current experimental limits on the axion parameter space

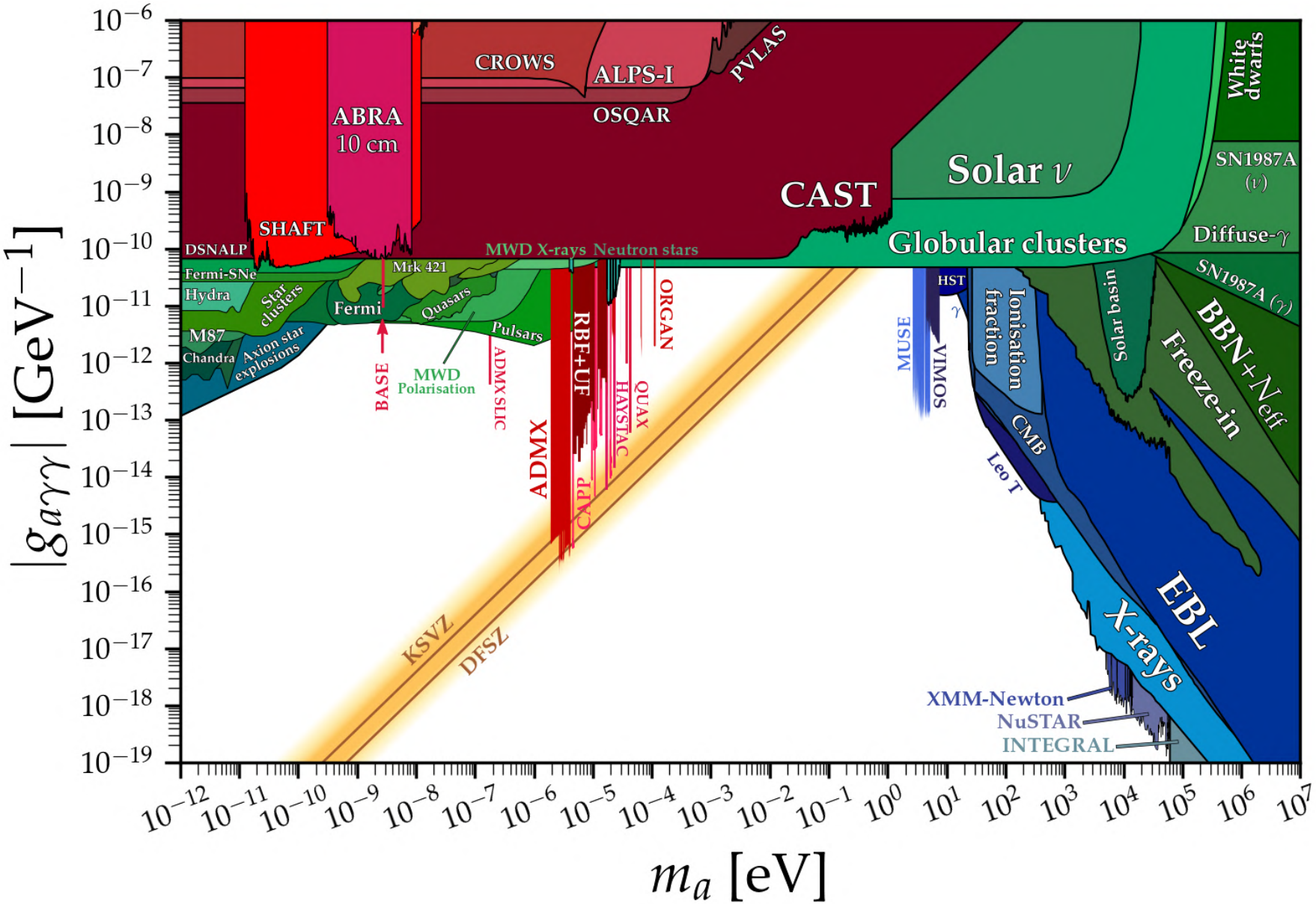

from https://cajohare.github.io/AxionLimits/

The haloscope: a resonant axion dark matter detector

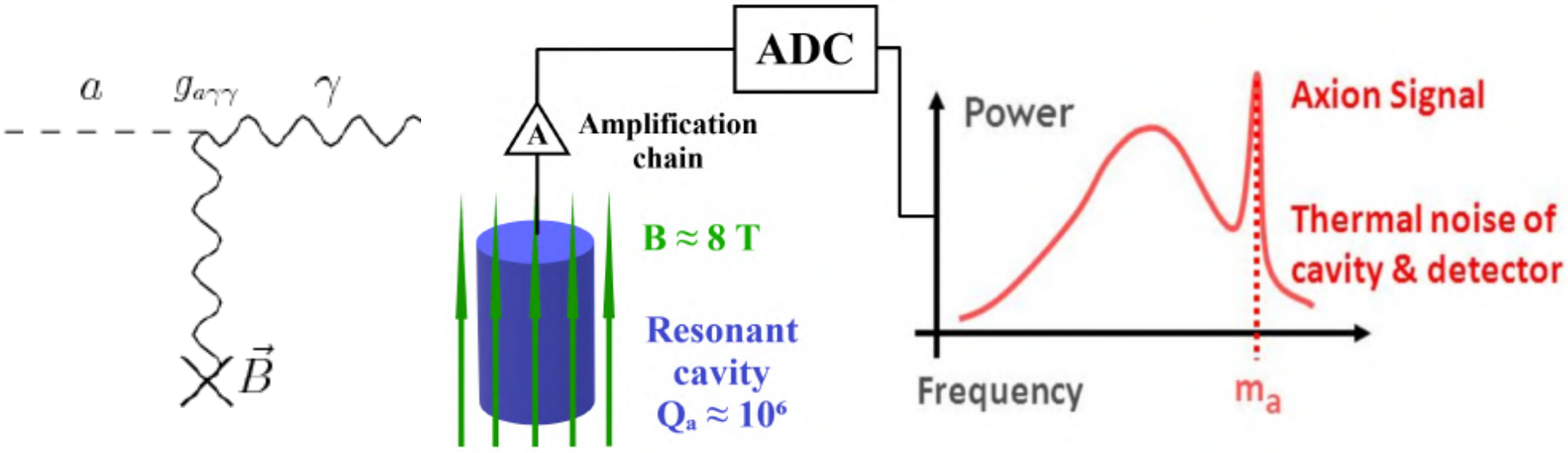

Axion signal is very narrow → We can collect and enhance it with resonant cavities!

- axions converted to photons inside intense magnetic field
- high-Q microwave cavity collects and integrates signal
- signal amplified by low noise receiver chain, then digitized by ADC
- axion signal revealed as excess power over noise fluctuations

Expected axion signal

The collected axion power extracted from the cavity is:

$$P_{axion} = \left(g_\gamma^2 \frac{\alpha^2}{\pi^2} \frac{\hbar^3 c^3 \rho_a}{\mu_0 \chi} \right) \left(\frac{\beta}{1+\beta} \omega_c B_0^2 \, V \, C_{nml} \frac{Q_L}{1 + \left(2 Q_L \frac{\delta \omega_a}{\omega_c} \right)^2} \right)$$

where the form factor C_{nml} is given by:

$$C_{nml} = \frac{\left(\int_V \mathbf{E_{nml}} \cdot \mathbf{B_{ext}^2} \, d^3x \right)^2}{\int_V \mathbf{B_{ext}^2} \, d^3x \cdot \int_V \epsilon \mathbf{E_{nml}^2} \, d^3x}$$

Then, substituting the parameters of our apparatus:

$$P_{axion} \approx 1.1 \cdot 10^{-23} \, W \left(\frac{V}{1.06 \, l} \right) \left(\frac{B}{8 \, T} \right)^2 \left(\frac{C}{0.028} \right) \left(\frac{g_\gamma}{-0.97} \right)^2 \cdot$$

$$\cdot \left(\frac{\rho_a}{0.45 \, GeV \, cm^{-3}} \right) \left(\frac{\nu_c}{10.35 \, GHz} \right) \left(\frac{Q_L}{300000} \right)$$

Noise background estimation

System noise → thermal noise + quantum noise + added noise:

$$P_{noise}(\Delta\nu) = N(\nu, T)h\nu\Delta\nu = \left[\left(\frac{h\nu}{e^{\frac{h\nu}{k_B T}} - 1}\right) + h\nu\left(\frac{1}{2} + N_A\right)\right]\Delta\nu = k_B T_{sys}\Delta\nu$$

But: $h\nu \sim 0.5$ K at 10 GHz, T$\sim$ 0.1 K for our apparatus → only small contribution from the physical temperature
Let us then suppose $T_{sys} \approx T + T_A \sim 2$ K and $\Delta\nu \approx 8.6$ kHz:

$$P_{noise} \approx k_B T_s \Delta\nu \approx 2.4 \cdot 10^{-19}\ W$$

Then, from the Dicke radiometer equation, the fluctuations after Δt total integration time are:

$$\sigma_{Dicke} \sim k_B T_s \sqrt{\frac{\Delta\nu}{\Delta t}} = 4.2 \cdot 10^{-23}\ W \left(\frac{T_{sys}}{2\ K}\right)\left(\frac{\Delta\nu}{8.6\ kHz}\right)^{\frac{1}{2}}\left(\frac{3600\ s}{\Delta t}\right)^{\frac{1}{2}}$$

Experimental apparatus

Cryostat technical scheme

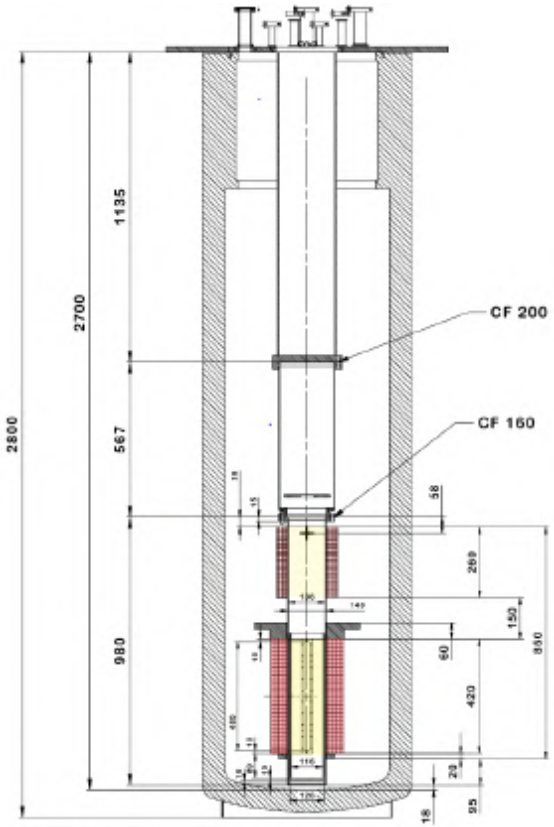

From left to right:

- Rack hosting the magnet current generator, thermometers and liquid helium level sensor
- Dewar containing the cryogenic part of the apparatus
- Vector Network Analyzer (VNA) used for reflection and transmission measurements
- Rack hosting signal generators, room temperature electronics and ADC
- Liquid helium supply

Cavity mountings and tuning mechanisms

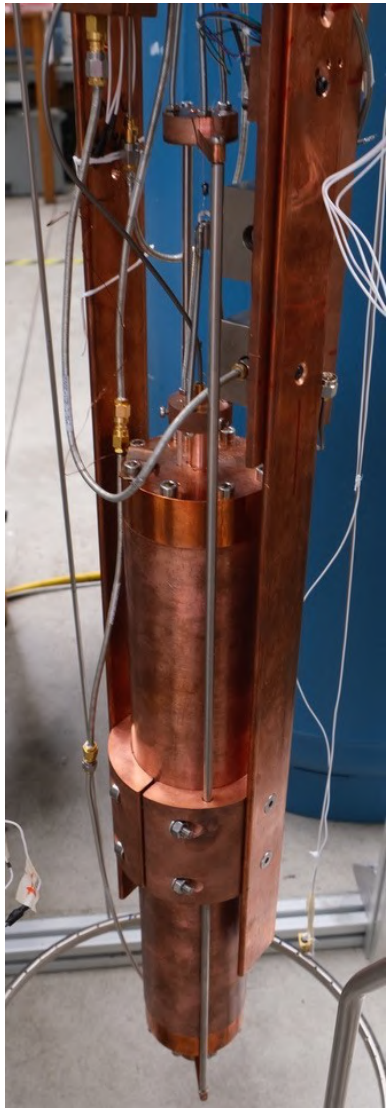

8T Magnet

The magnet is powered by a 125 A custom-built, ultra-high precision current generator

Compensation coil shields the cryogenic electronics from $\sim$ 0.3 T residual field

Nb-Ti SC magnet surrounds the cavity and provides the 8T magnetic field

Measured central field constant	869.152	Gauss/Ampere
Homogeneity in 10mm DSV	< 0.1	%
Design Field at 4.2K	8	Tesla
Current for 8 Tesla	92.04	Ampere
Maximum field tested at 4.2K	8.1	Tesla
Nominal Inductance	$\sim$ 61	Henry
Recommended switch heater voltage	2.5	Volt
Suggested nominal energization rate for 0-3T	0.07	Ampere/second
Suggested nominal energization rate for 3-6T	0.06	Ampere/second
Suggested nominal energization rate for 6-7T	0.05	Ampere/second
Suggested nominal energization rate for 7-8T	0.04	Ampere/second
Resistance across terminals at room temperature	$\sim$ 26.3	Ohm
Switch heater (1) resistance (Black wires)	$\sim$ 103.8	Ohm
Switch heater (2) resistance (Red wires)	$\sim$ 103.1	Ohm

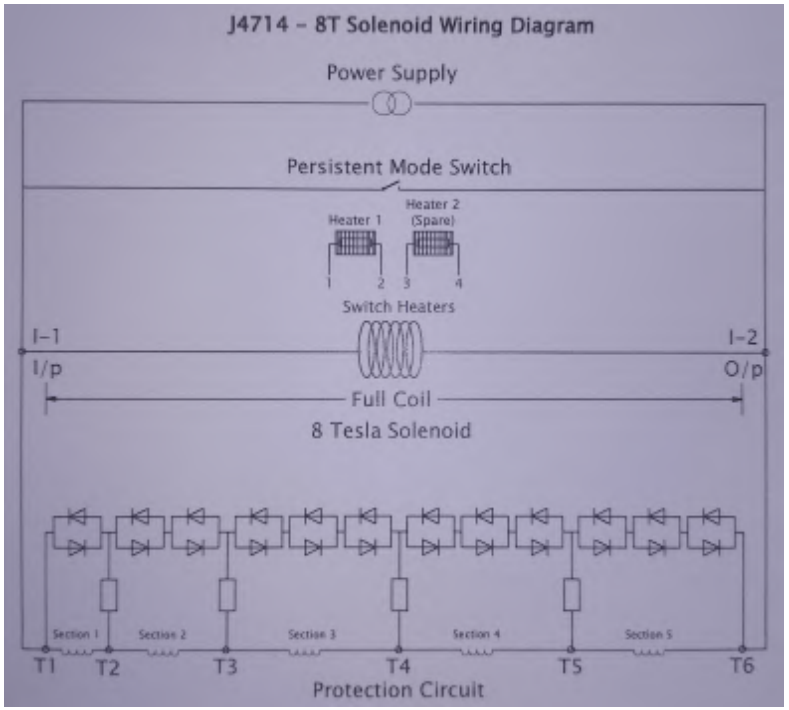

The high-Q dielectric cavity

- exploiting the **TM_{030}** mode
- high-Q factor due to field confinement by dielectric shells
- simple tuning mechanism allows frequency adjustment over a 1.2 MHz range
- Q factor stays high over the whole range, no mode disturbances seen

R_{cav}	28.55
R_{cyl_1}	10.88
R_{cyl_2}	20.90
t_{cyl_1}	2.35
t_{cyl_2}	1.94
h_{cone}	6.00
h_{cav}	420

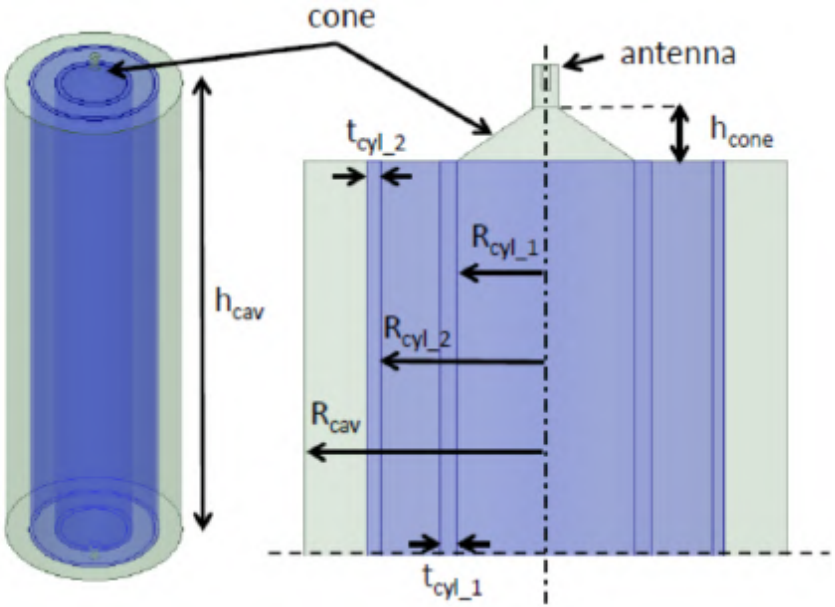

Cavity	ν_{cav}	V	C_{nml}	$V_{eff}=C\cdot V$	Q_0
QUAX 2020	10.4 GHz	80 cm^3	0.69	55.6 cm^3	76000
QUAX 2022	10.35 GHz	1056 cm^3	0.033	34.7 cm^3	$9.1\cdot10^6$

→ described in 10.1103/PhysRevApplied.17.054013

Electric field and surface loss for the TM_{030} mode

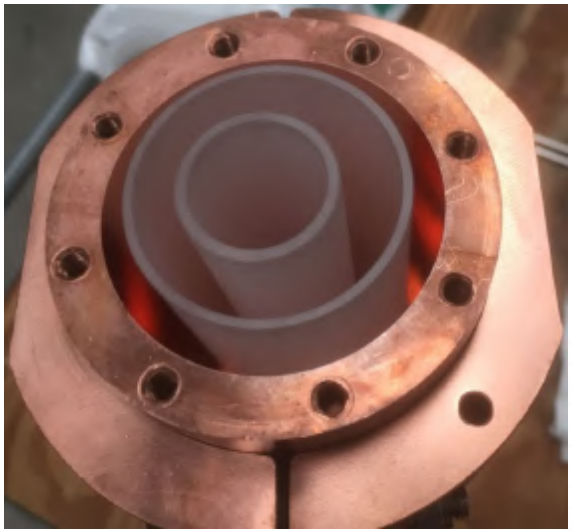

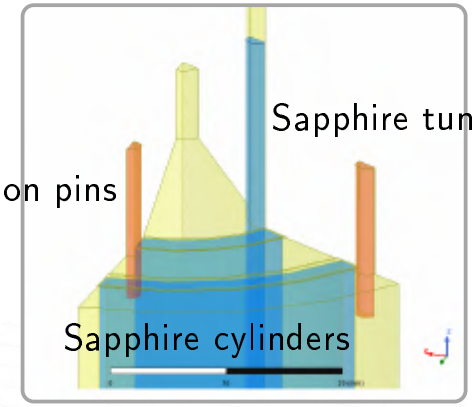

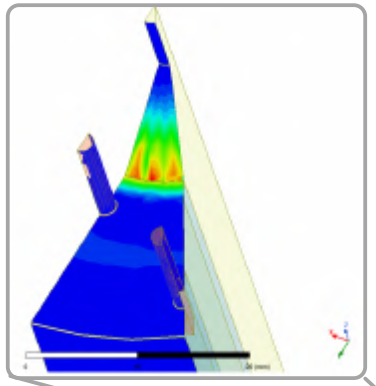

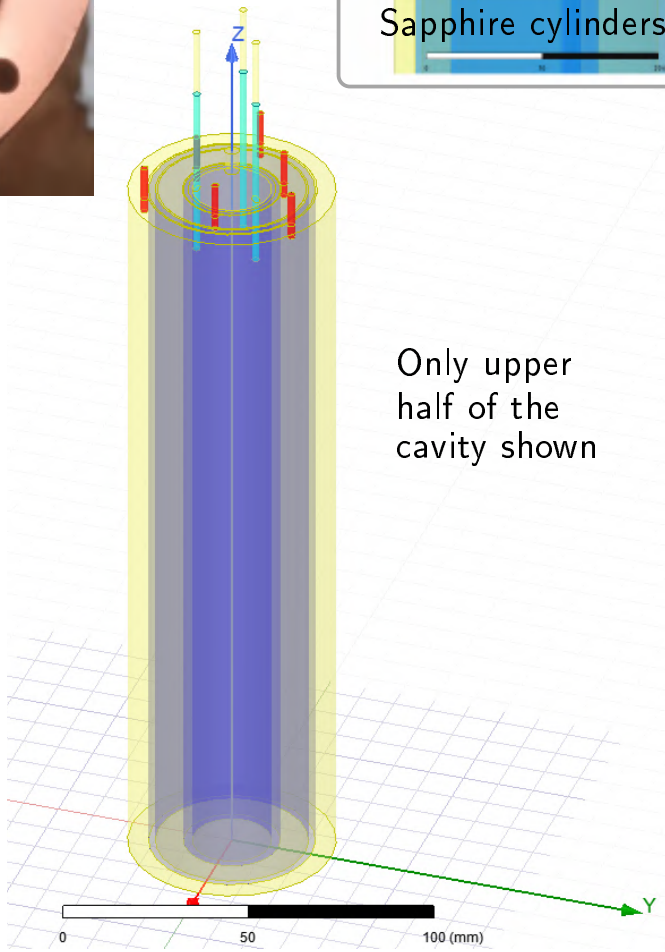

Only upper half of the cavity shown

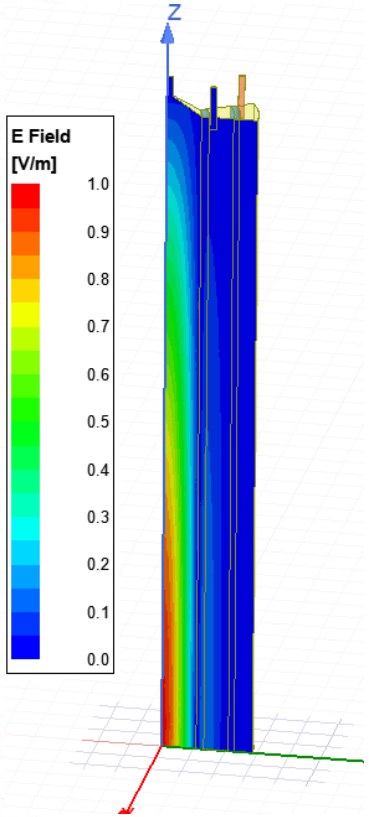

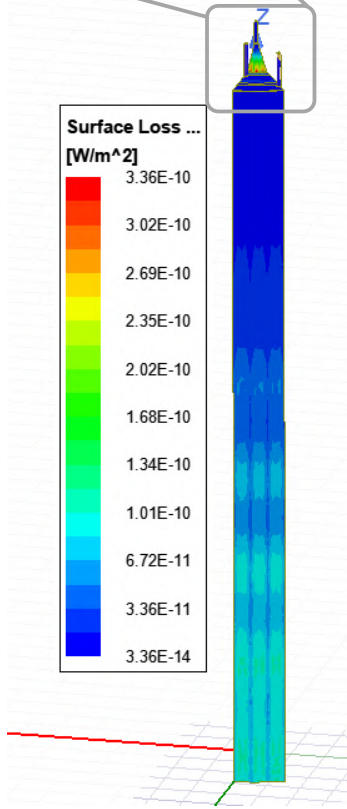

Cryogenic RF setup

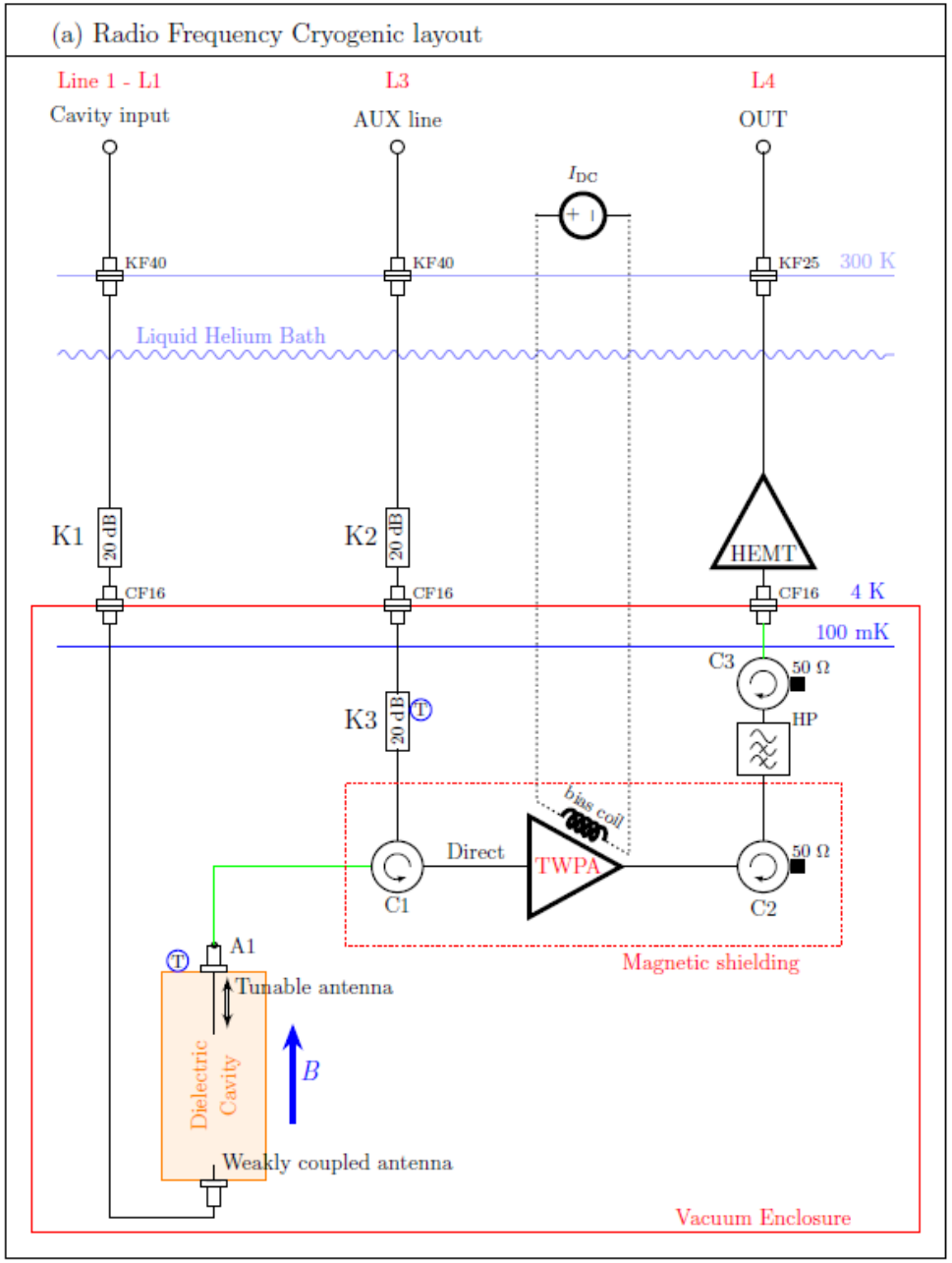

Picture of the cryogenic part of the receiver prior to TWPA installation

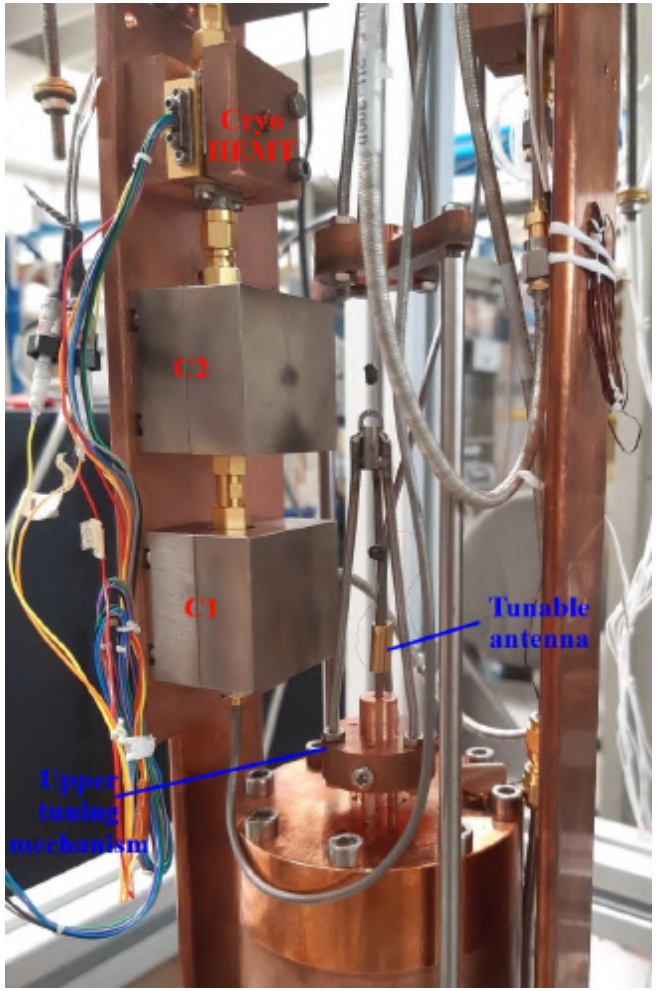

Room temperature electronics

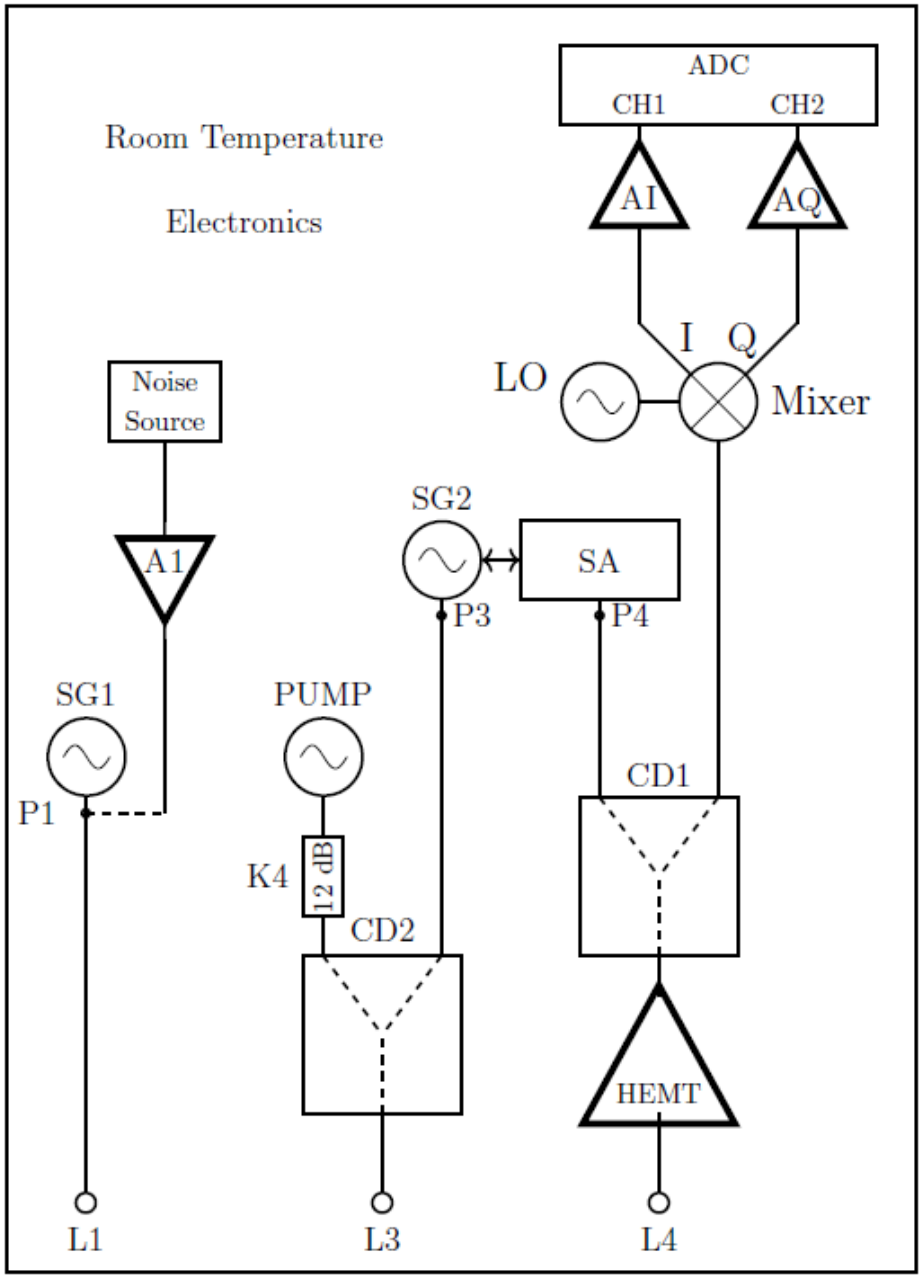

- Piloting the external source SG2 with the Spectrum Analyzer allows to obtain cavity parameters from reflection fit of **S43** (i.e. input on line 3, output on line 4) $\rightarrow \nu_{cav}$, Q_L, β
- The amplified 10^4 K diode noise source allows to obtain indipendent measurement of ν_{cav} and Q_L from **S41**
- SG2 also allows to add off-resonance monochromatic tone to monitor gain stability during data runs
- Data acquisition during runs handled by ADC
- All instruments referenced to GPS-disciplined clock

TWPA amplifier

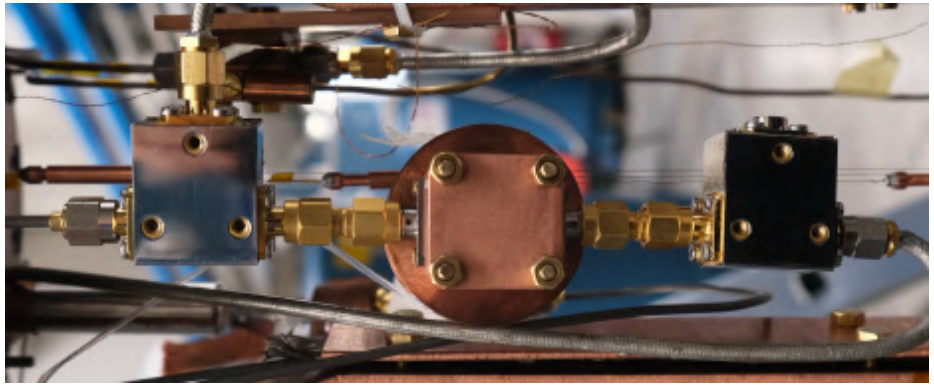

- Provided by **Grenoble INP group**
- Based on three-wave mixing, provides extremely wide-bandwidth amplification
- Tested repeatedly to ensure temporal stability and effective magnetic shielding
- Minimum T_{sys} obtained on frequency-tunable $\sim$ 1 MHz-wide maximum gain lobes

n	Magnetic field (T)	Cavity Temp. (K)	T_{sys} (K) On Res.	K3 Temp. (K)	T_{sys} (K) Off Res.
1	0	0.12	2.12 ± 0.05	0.18	2.22 ± 0.06
2	0	0.12	2.04 ± 0.03	0.19	1.94 ± 0.03
3	4.0	0.13	2.11 ± 0.03	0.22	2.16 ± 0.03
4	0	0.12	1.89 ± 0.04	0.18	1.98 ± 0.05
5	8.0	0.11	2.23 ± 0.06	0.18	2.26 ± 0.06

$\rightarrow$ previous model described in 10.1063/5.0098039

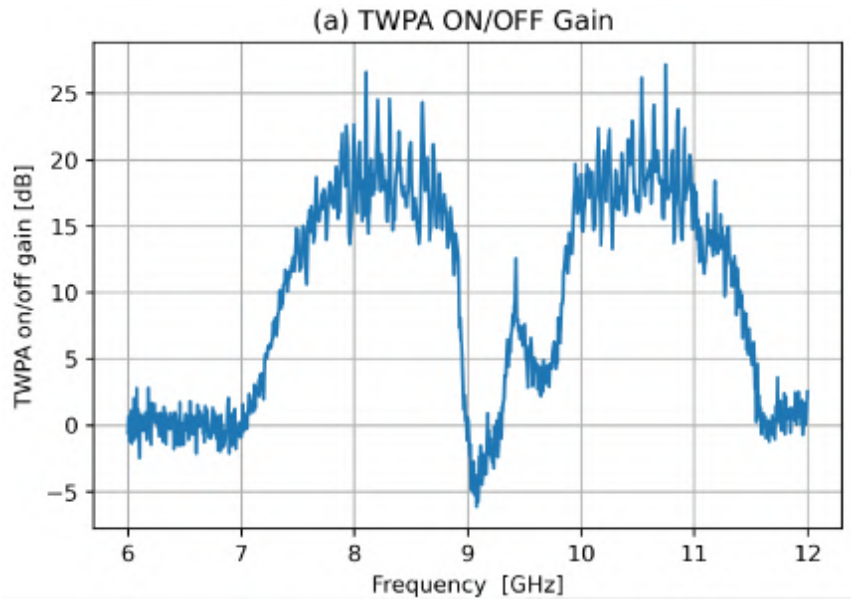

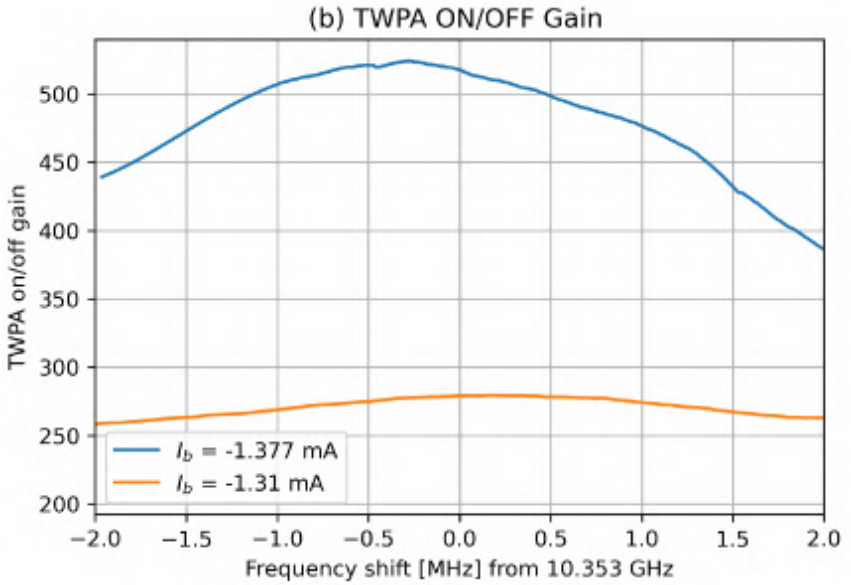

Calibration procedure

The calibration procedure exploits the presence of three lines and is a two step process:

- First we calibrate the transmission G of the lines (the K are the VNA transmission measurement results):

$$\begin{cases} G_1 = \frac{K_4 1 + K_1 3 - K_4 3}{2} \\ G_3 = \frac{-K_4 1 + K_1 3 + K_4 3}{2} \\ G_4 = \frac{K_4 1 - K_1 3 + K_4 3}{2} \end{cases} \rightarrow \begin{cases} G_1 = (-74.7 \pm 0.1)\, dB \\ G_3 = (-50.9 \pm 0.1)\, dB \\ G_4 = (+52.1 \pm 0.1)\, dB \end{cases}$$

- Secondly we measure the noise level at the cavity tunable antenna through the Y-factor method:

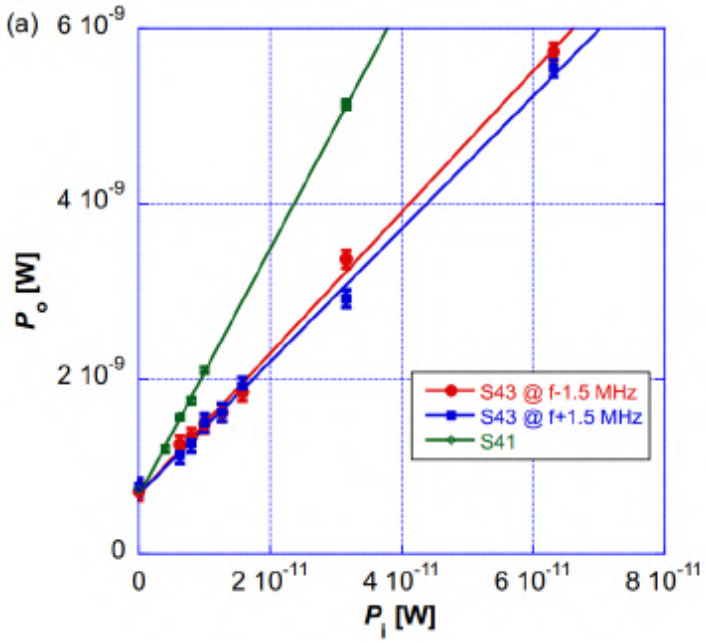

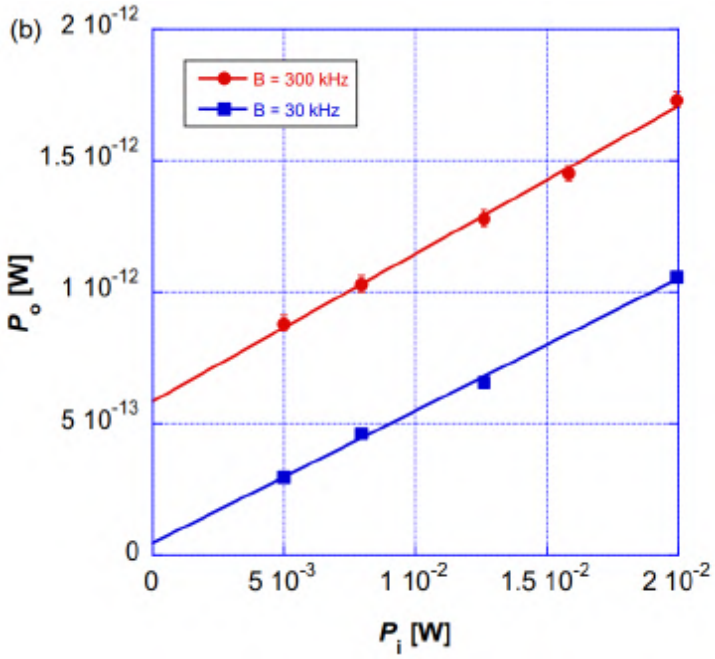

Noise contributions breakdown

We have $T_{sys}^{avg} = 2.06 \pm 0.13$ K on resonance, and $T_{sys}^{avg} = 2.07 \pm 0.14$ K off resonance.

Errors dominated by spread of the points → significant long term temperature variations

Noise contributions modeled at the HEMT output in the following general way:

$$PSD_{HEMT}(\nu_s) = h\nu_s G_{HEMT}[N_{HEMT} + (1-\Lambda_2)N_2 + \Lambda_2 G_{TWPA}(N_{TWPA}$$

$$+(1-\Lambda_1)N_1 + \Lambda_1 N(\nu_s; T_s) + \Lambda_1 N(\nu_i; T_i))]$$

We know the transmissions $\Lambda_{1,2}$ of the non-superconductive cables to be almost 1, and G_{HEMT} to be high; then, at the input point (3-wave mixing → the idler also adds noise):

$$N_{sys} \simeq N(\nu_s, T_s) + N(\nu_i, T_i) + \frac{N_{TWPA}}{\Lambda_1} + \frac{N_{HEMT}}{\Lambda_1 \Lambda_2 G_{TWPA}}$$

where N_{HEMT} can be estimated from the noise temperature of the system with TWPA off.

Term	Value (K)	N photons
$N(\nu_s, T_s)$	0.27	0.5
$N(\nu_i, T_i)$	0.27	0.7
$N_{\mathrm{HEMT}}/\Lambda_1\Lambda_2 G_{\mathrm{TWPA}}$	0.39	0.8
N_{sys}	2.06	4.2
$N_{\mathrm{TWPA}}/\Lambda_1$		2.2

Run data-taking procedure

- The cavity frequency is readjusted monitoring the cavity resonance with the VNA on the S→B path
- A reflection spectrum is acquired using the VNA on the A→B path: this allows us to calculate the coupling β of the antenna
- The spectrum of the resonance is measured by feeding the input of the S→B line with an amplified 10000 K noise source, and acquiring the output on the ADC for ∼423.7 s → we obtain frequency and loaded quality factor of the resonance
- A data run with no input signal is acquired on the ADC. Measured liquid helium level and cavity temperature at the time the run is started are also recorded
- Being the cavity-LO detuning always ∼ 500 kHz, the employed 2 MHz sampling rate allows to reconstruct the cavity signal from the acquired time series by the Nyquist-Shannon theorem

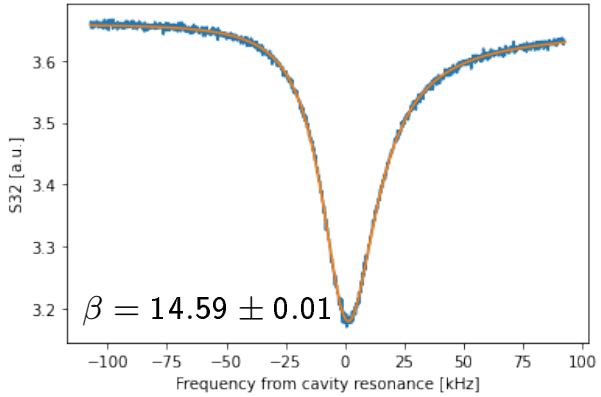

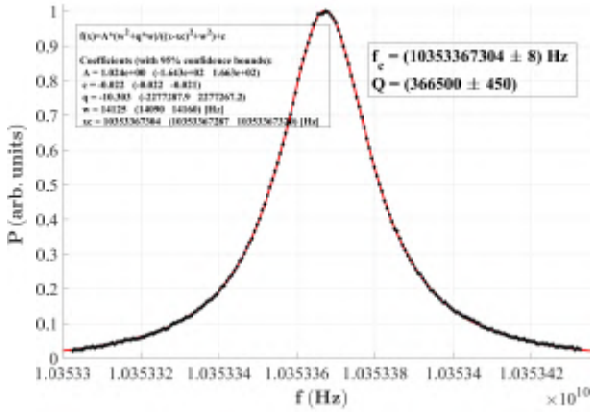

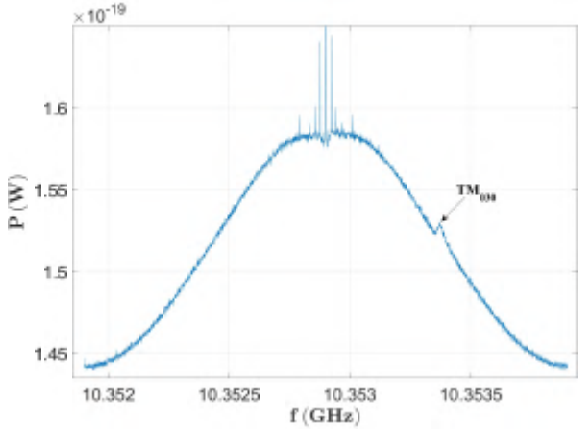

Run parameters overview

- 8 runs acquired over the span of 17 consecutive hours
- Antenna massively overcoupled to maintain a loaded Q factor close to 1/4 of the axion one, allowing to apply standard analysis procedure and increase signal extraction efficiency
- Q_0 estimated from measurements at high antenna coupling lower than expected!

RUN n	ν_c (GHz)	Duration (s)	T_c (mK)	T_{K3} (mK)
389	10.353 525	2000	113	177
392	10.353 499	2000	111	178
394	10.353 473	2000	112	181
395	10.353 473	4000	113	185
397	10.353 444	2000	114	182
399	10.353 424	4800	112	177
401	10.353 399	28000	110	176
404	10.353 368	2000	110	176

RUN n	$\nu_c - 10.353$ GHz (Hz)	Cavity Q_L	β	Ref Peak (a.u.)
389	522 600	230 000	10.9	179
392	494 100	240 000	12.0	185
394	468 800	245 000	12.2	186
395	468 800	245 000	12.2	187
397	439 800	245 000	11.4	175
399	418 500	245 000	11.4	191
401	393 100	250 000	11.4	186
404	365 400	255 000	11.9	193

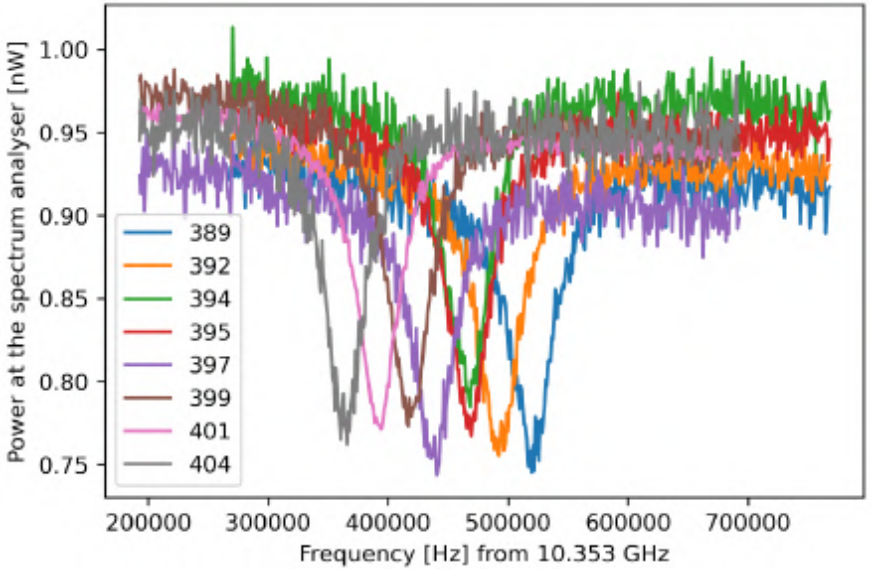

Raw data processing

- Mean spectra obtained by the Bartlett method of averaging periodograms, bin size is chosen as $\Delta\nu = 651$ Hz
- The off-resonance monitoring peak amplitudes are subsequently retrieved from the obtained power spectra, showing gain stability within 5.3%
- For each run, we obtain β fitting the cavity reflection collected on the SA on the S43 line
- Similarly, we obtain ν_{cav} and Q_L from a Lorentzian fit of the excess noise transmitted through the cavity with diode noise source on and acquired on the ADC
- Due to insufficient high frequency noise rejection from the ADC filters, noise levels are increased by aliasing by a factor of $\sim$1.7 during the digitization.

$\rightarrow$ For all ADC data, the temperature of the cavity appears as $T_{sys}^{ADC} = 1.7 \cdot T_{sys} = 3.5$ K!

Data analysis: Axion detection procedure

Detection algorithm based on classical hypothesis testing framework: on the basis of the observed data, is the null hypothesis (only noise) rejected or not when compared with the alternative hypothesis (signal + noise)

Solution: set threshold, and use ML (maximum likelyhood criterion) to implement decision rule... but very robust model of the noise background is needed

We thus model PSD at haloscope output as a first order polynomial ratio:

$$F(\nu) = e^2 \cdot \frac{|\nu - a + ib|^2}{|\nu - c + id|^2} + f \cdot (\nu - c)$$

We fit every run in a 200 bin window about the cavity frequency. However: quality of the fits degrades with too long integration times!

$\rightarrow$ all longer runs sliced into subruns of 2000 s duration, then recombined after fitting by weighed mean

Now, quality of fits is good; with the employed choice of $P_\alpha(\chi^2)<0.001$ to reject the null hypothesis, no candidates are flagged

Data analysis: upper limit on axion-photon coupling /1

- No candidate signals found → a grand spectrum is built, again by combining all bins of the same frequency using the error on each bin as weight
- $\min(\sigma_{res,G.S.}) = (6.2 \pm 0.4) \cdot 10^{-24}$ W, compatible with Dicke estimate of $(6.5 \pm 0.4) \cdot 10^{-24}$ W
- $\chi^2 = 452$ over 442 bins → $P(\chi^2)$=0.37, H_0 not rejected → proceed for the upper limit

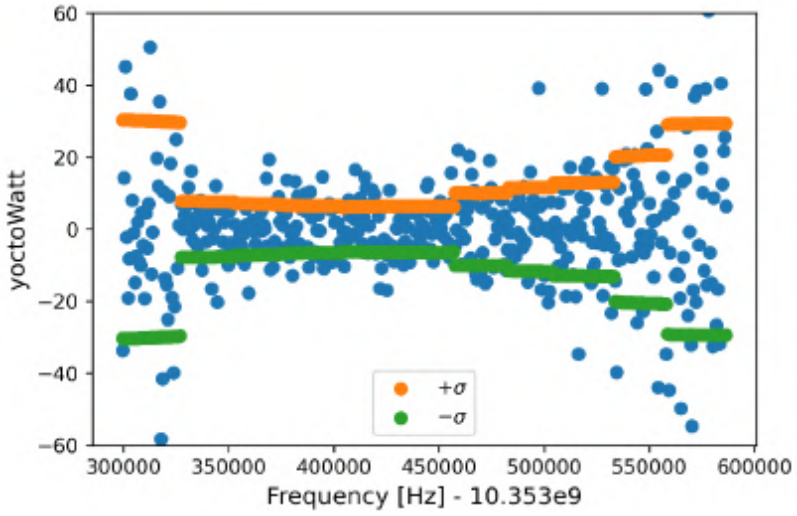

We assume for the axion the standard halo model with $\rho_a = \rho_{DM}$ and Maxwell-Boltzmann energy distribution $f_a(\nu, \nu_a)$

$$f_a(\nu, \nu_a) = \frac{2}{\sqrt{\pi}} \sqrt{\nu - \nu_a} \left(\frac{3}{1.7 \nu_a \langle \beta_a^2 \rangle} \right)^{3/2} e^{-\frac{3(\nu - \nu_a)}{1.7 \nu_a \langle \beta_a^2 \rangle}}$$

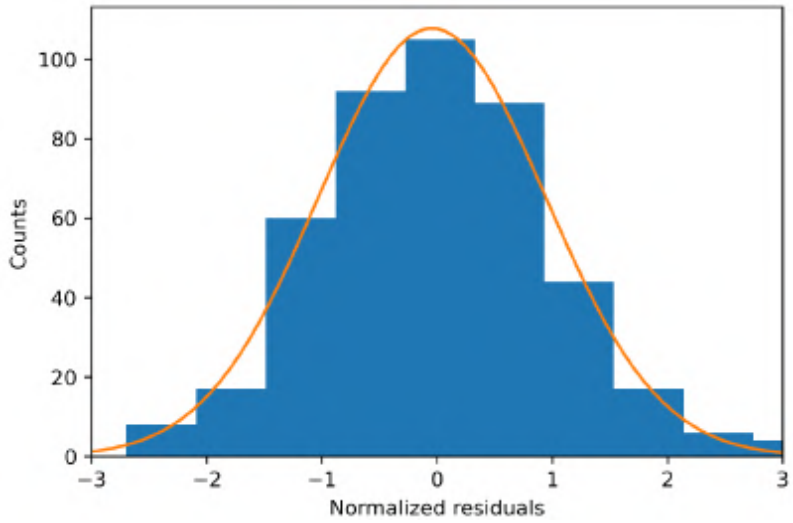

Data analysis: upper limit on axion-photon coupling /2

The axion power spectrum is:

$$S_a(\nu, \nu_a, \nu_{cav}) = g^2_{a\gamma\gamma} \frac{\hbar^3 c^3 \rho_a}{m_a^2} \frac{2\pi \nu_{cav} B_0^2 V C_{030}}{\mu_0} \times$$

$$\times \frac{\beta}{1+\beta} \cdot \frac{Q_L}{1 + \left(2 Q_L \frac{\nu - \nu_{cav}}{\nu_{cav}}\right)^2} \cdot f_a(\nu, \nu_a)$$

- The subruns are discretized into 33 intervals of center frequencies ν_i, and each subrun is fitted with the function $F(\nu_i) + S_a(\nu_i; \nu_a; \nu_{cav})B$, leaving $g^2_{a\gamma\gamma}$ as free parameter
- Monte Carlo simulations employed to check that the correct value was extracted by the procedure, by injecting synthetic signals in our data
- The values of $g^2_{a\gamma\gamma}(\nu_i)$ obtained from the subruns are then averaged together, using the uncertainties obtained from the fitting procedures as weights
- This in turn allows to set an upper limit on $g^2_{a\gamma\gamma}(\nu_i)$ at 90 % C.L.
- power constrained procedure adopted for the values of $g^2_{a\gamma\gamma}$ fluctuating below $-\sigma_{g_{a\gamma\gamma}}$

Run analysis results

We set a 90% Confidence Level upper limit on $g_{a\gamma\gamma}$ in the range 42.8178 - 42.8190 μeV, with peak sensitivity $g_{a\gamma\gamma}^{CL} < 2.05 \times 10^{-14}$ GeV^{-1}.

However, we couldn't exploit the full potential of the cavity and had to work at very high β:

The efficiency gets drastically lower if the cavity linewidth gets close to the axion width

$\rightarrow$ Very high-Q cavities only convenient in practice with (noiseless) single-photon counters, and/or when the temperature of the system can be controlled exceptionally well

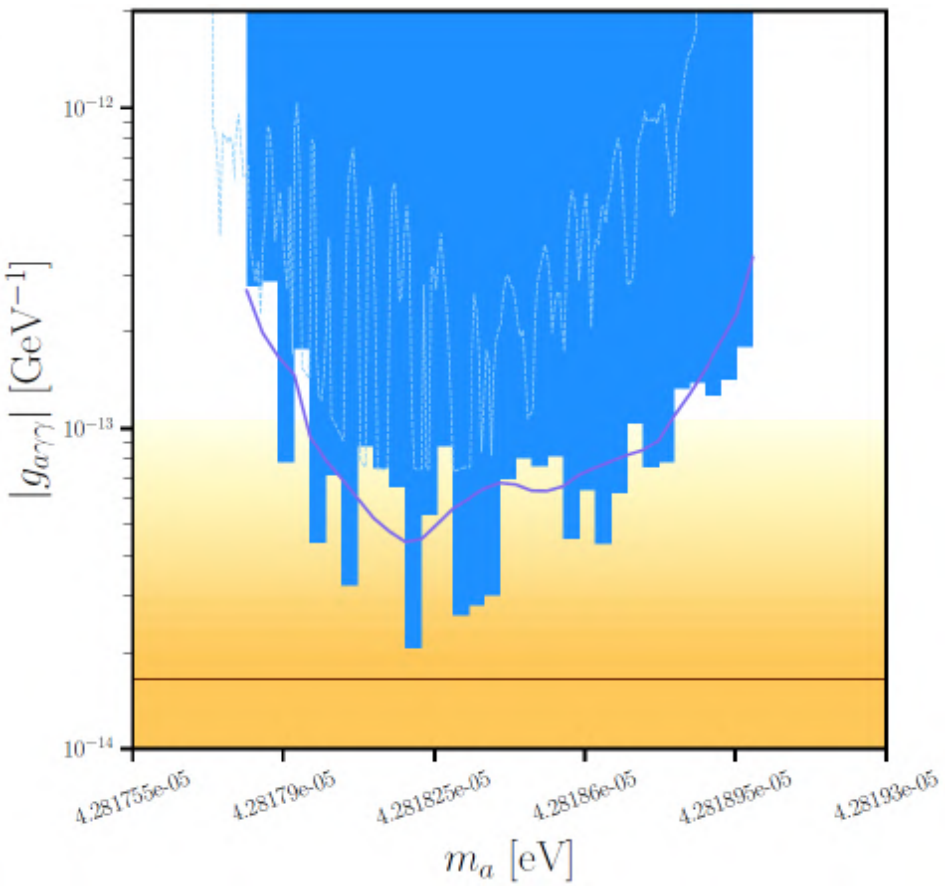

TM_{010} tunable clamshell cavity

- Alternative solution to tuning bars for empty cylindrical TM_{010} cavities
- Idea: tune the frequency by rotating one half of the cavity with respect to each other
- Radiative losses are negligible until very high aperture angles
- No degradation of Q expected for cavities with high aspect ratio

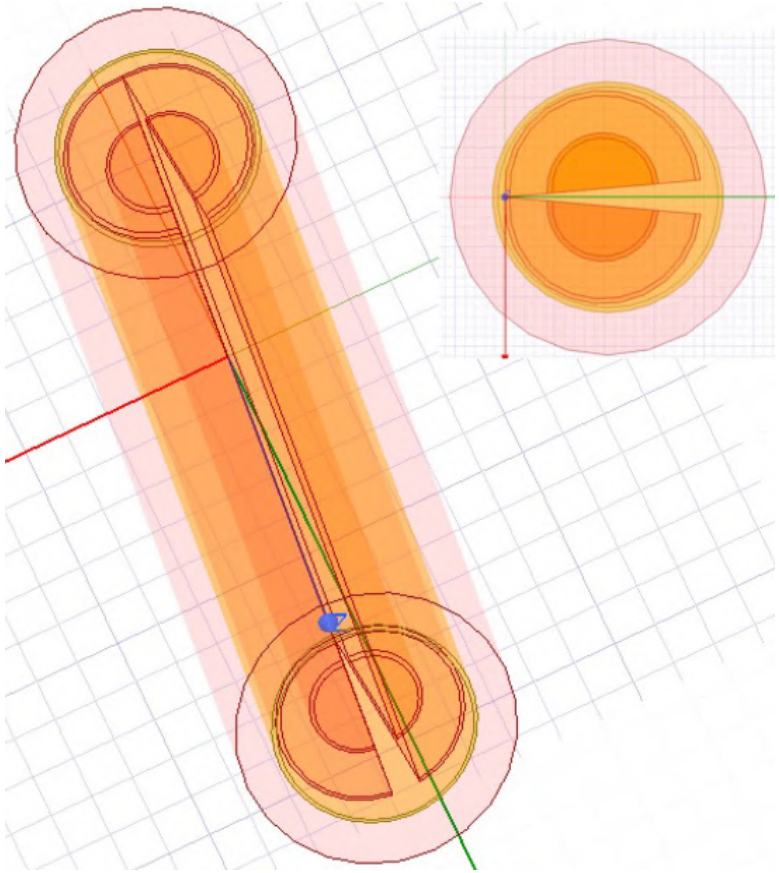

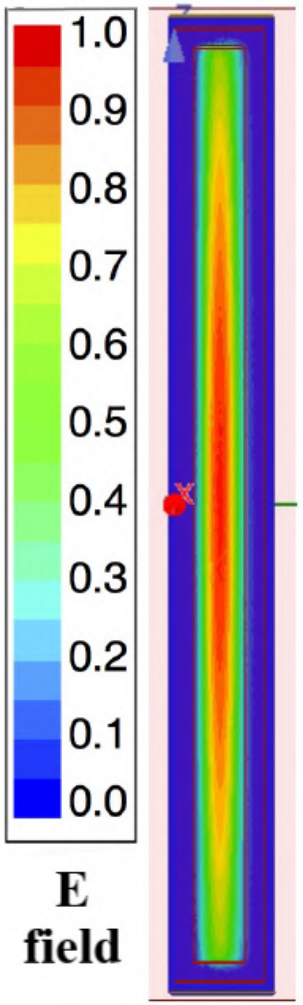

doi.org/
10.1063/
5.0137621

Simulations and experimental results

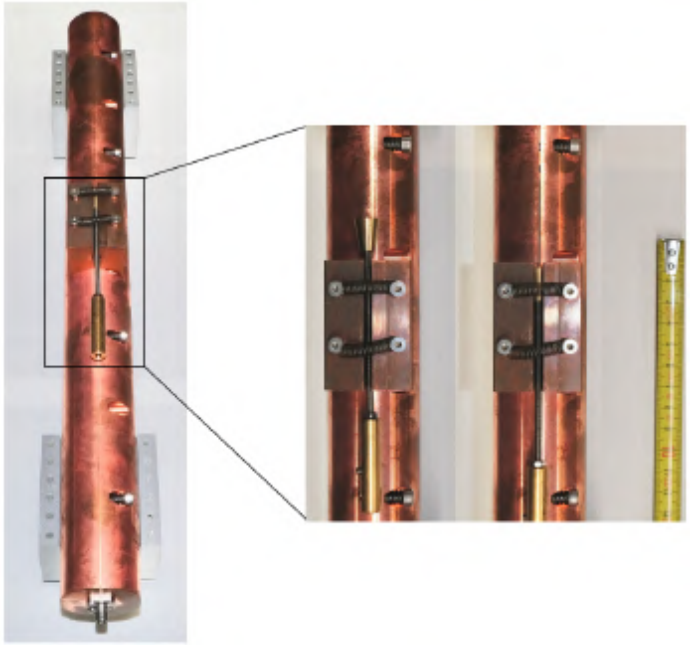

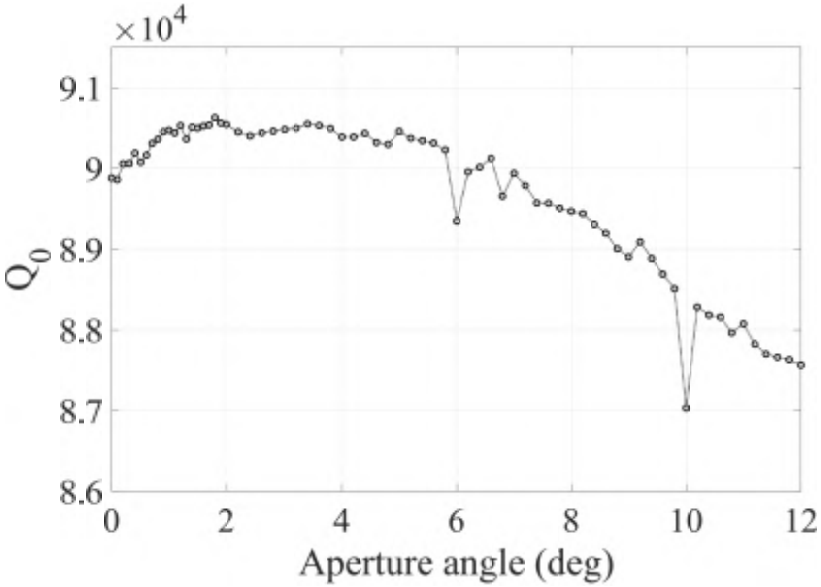

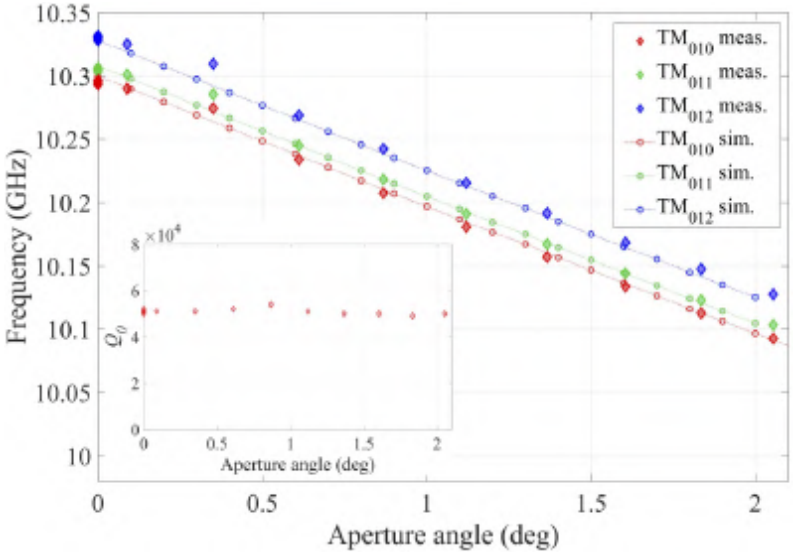

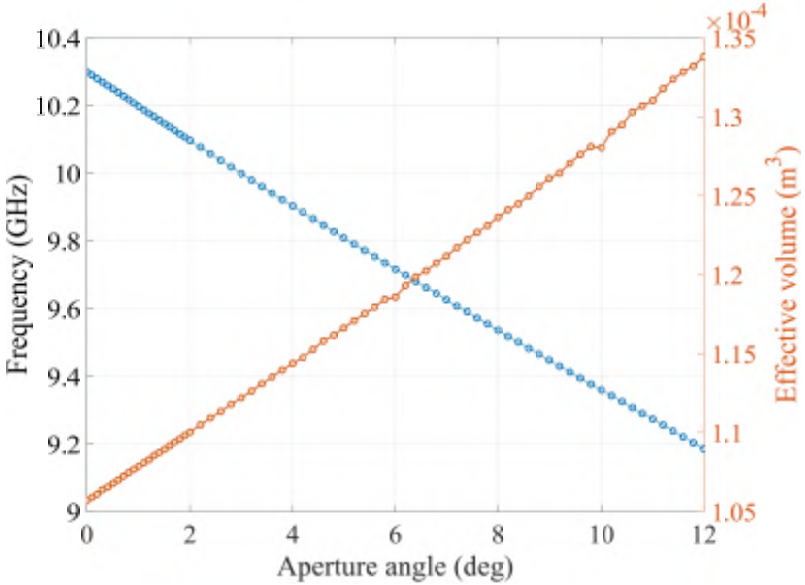

TM_{010} polygonal coaxial cavity: basic concept

COMING SOON ON ARXIV!

- High cavity volumes needed to extend haloscope approach to higher frequencies
- Idea: perfectly coaxial circular cavity → allows volume scaling to go as $\mathbf{r}^{-1}$
- Analogy with infinite rectangular cavity → expected C factors of the order of 0.8 for TM_{010} mode
- Tuning obtained by breaking continuous symmetry with a polygonal design allowing reciprocal rotation

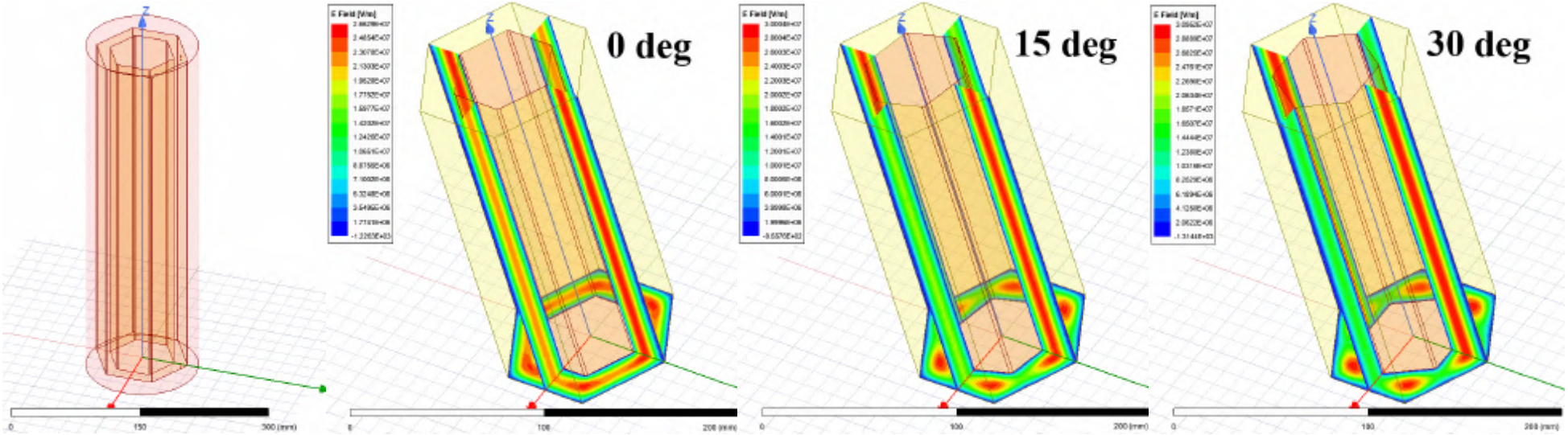

Simulations for ideal cavity model: mode map and expected parameters

- We employ a smaller h_{cav}=50 mm ideal cavity model
- Mode map obtained over the whole tuning range via Ansys HFSS drivenmodal simulation, Q and C obtained with eigenmode simulations
- Very high C>0.5 retained, but: eigenmode result not reliable for this kind of cavity!

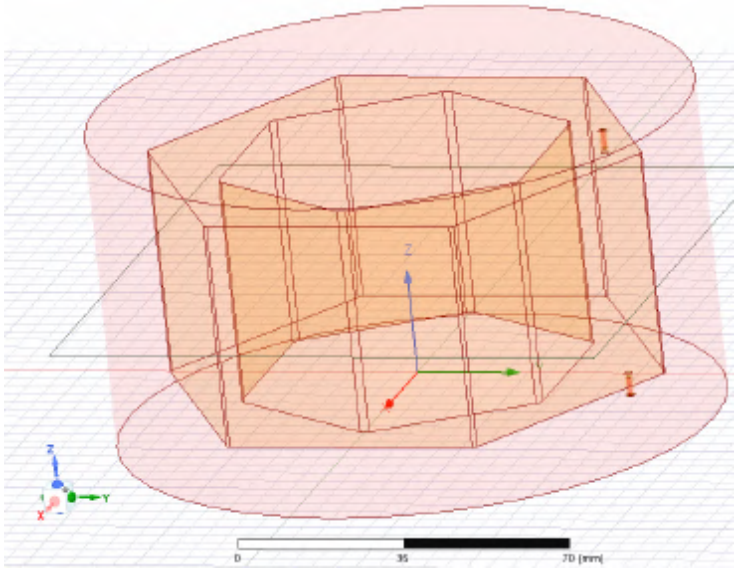

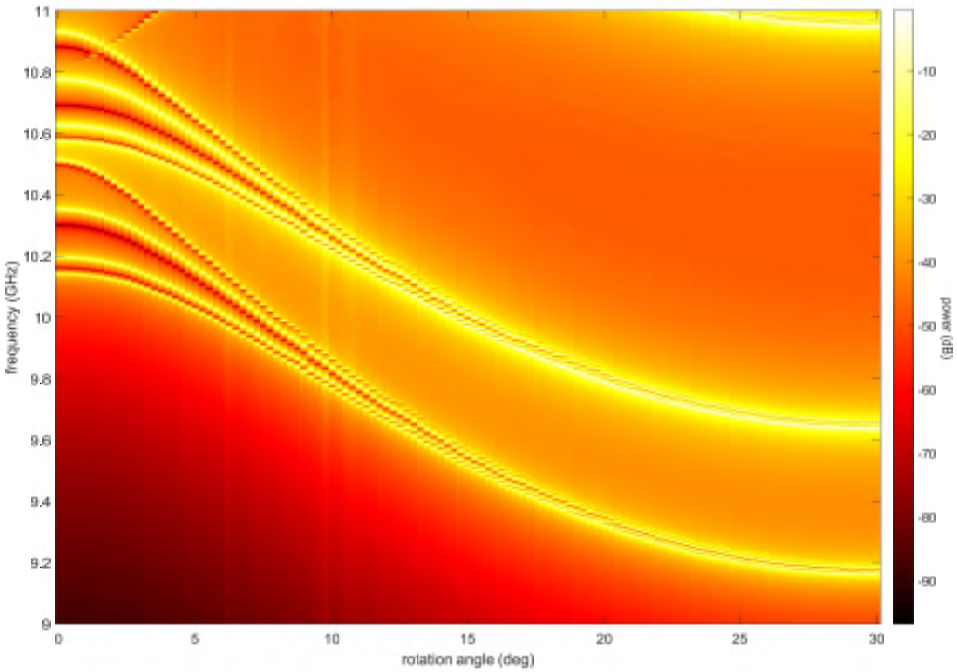

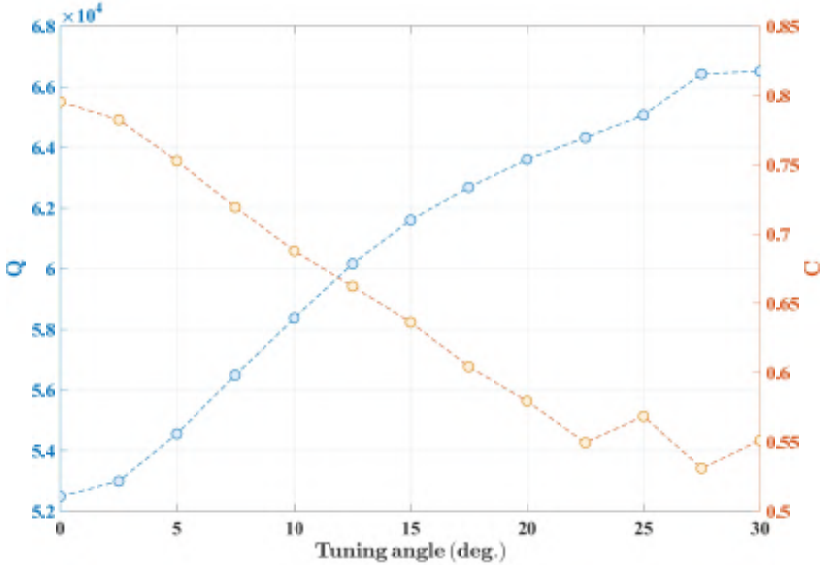

Influence of sides number and eigenmode-drivenmodal comparison

- We vary the number of prism sides leaving the inner and outer radius of the prisms constant
- Base resonant frequency changes → we normalize the frequency shift to obtain more relative comparison
- C calculated in both eigenmode and drivenmodal for the same configurations... different results obtained!

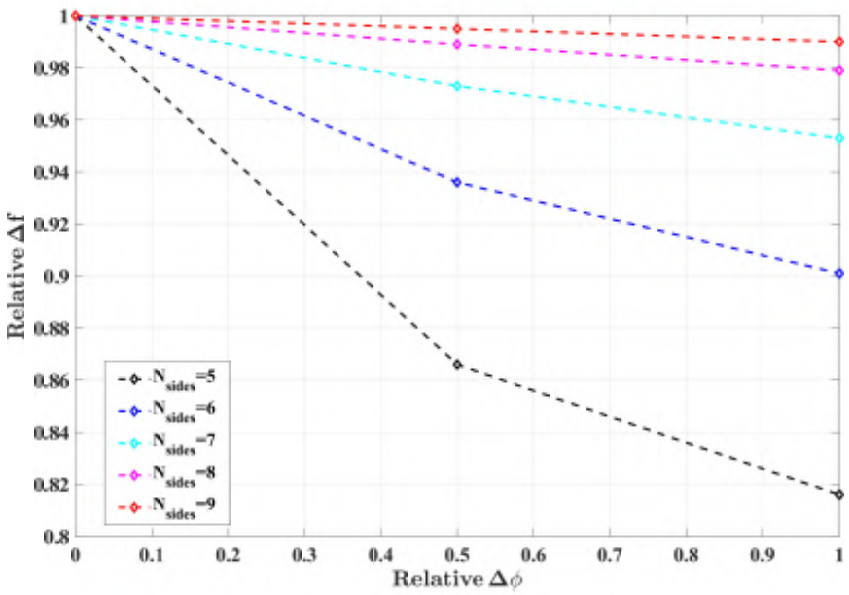

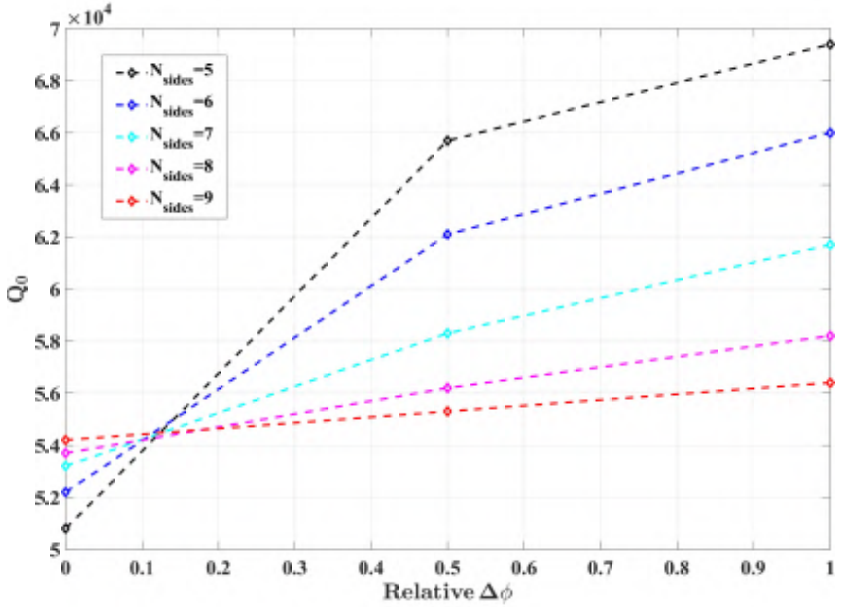

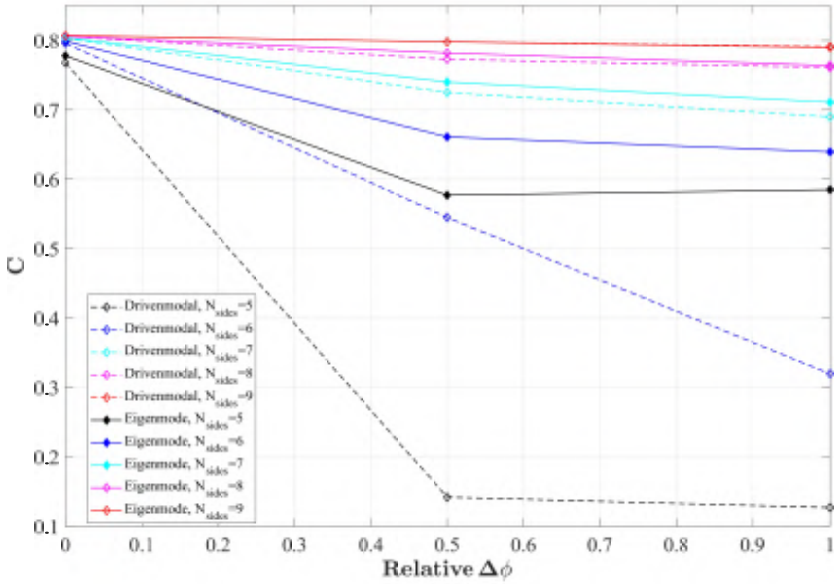

Cavity nonidealities: effect of translational misalignment

– Central prism translated with respect to the external one along one diagonal

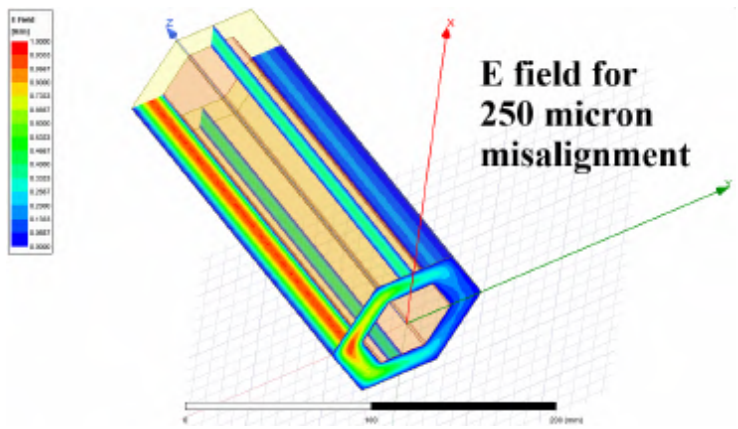

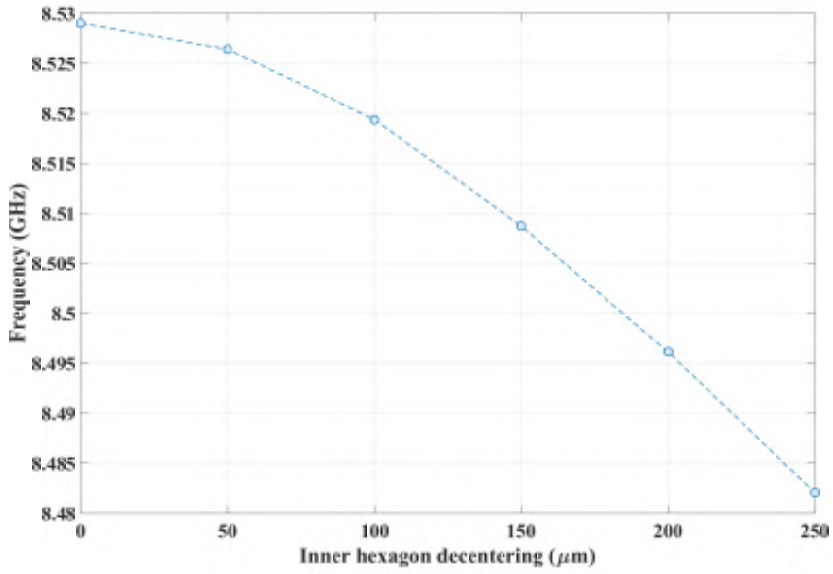

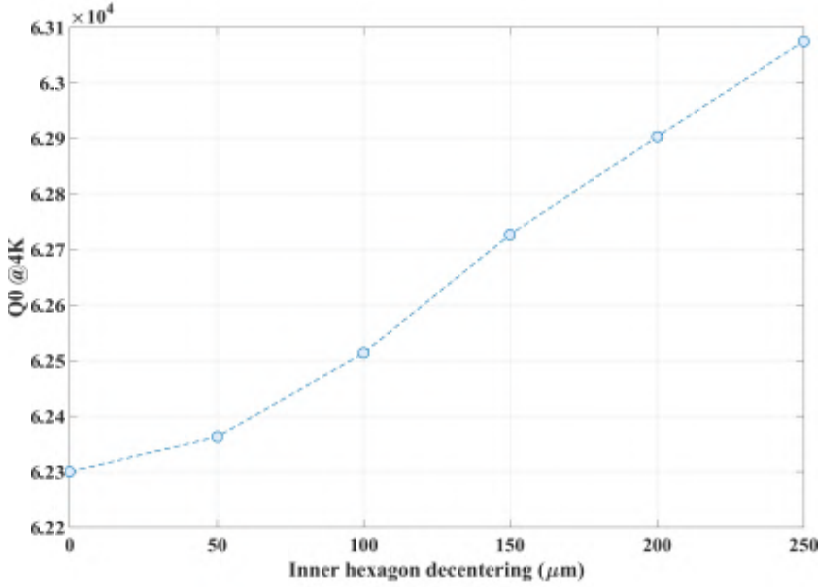

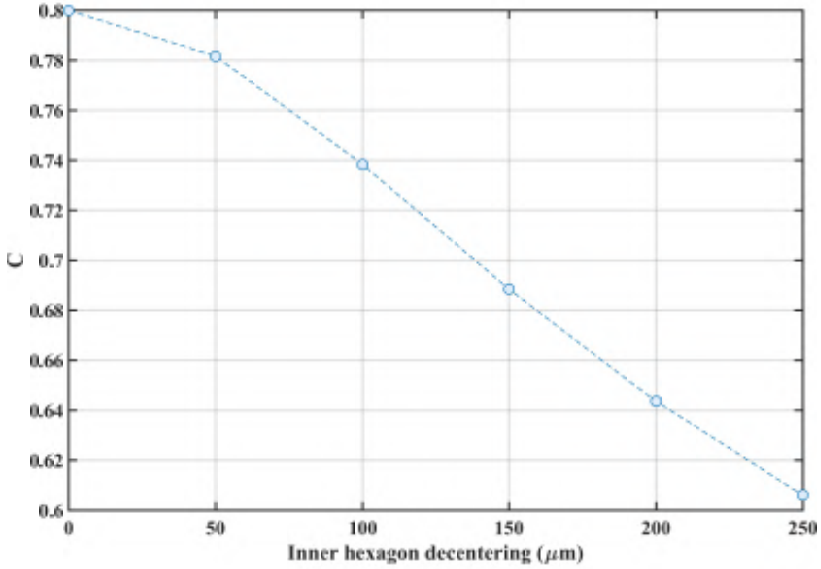

Cavity nonidealities: effect of prism tilt

– Central prism tilted with respect to the external one along a diagonal

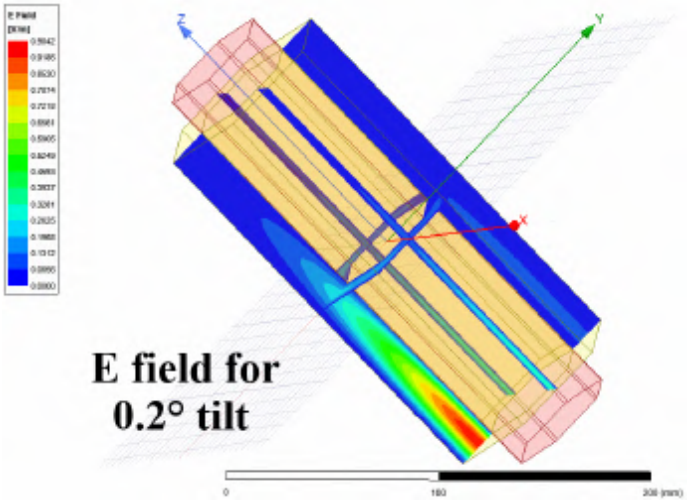

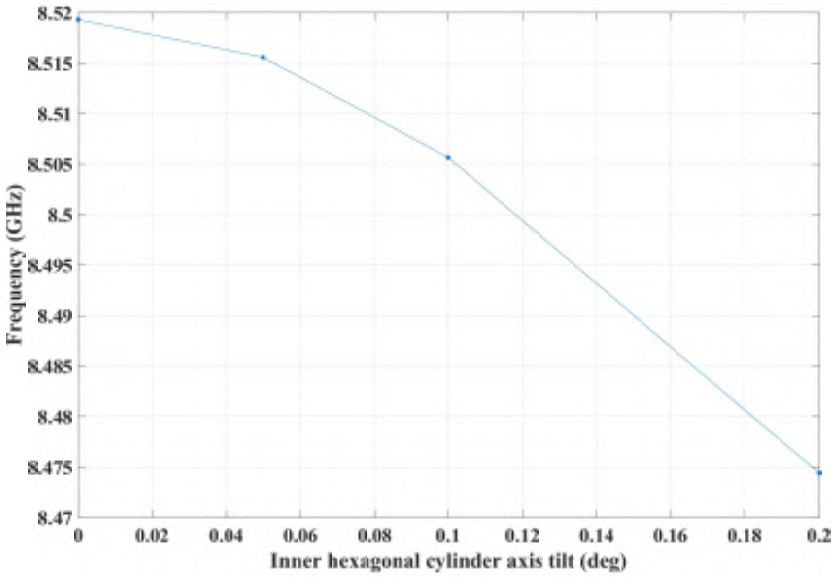

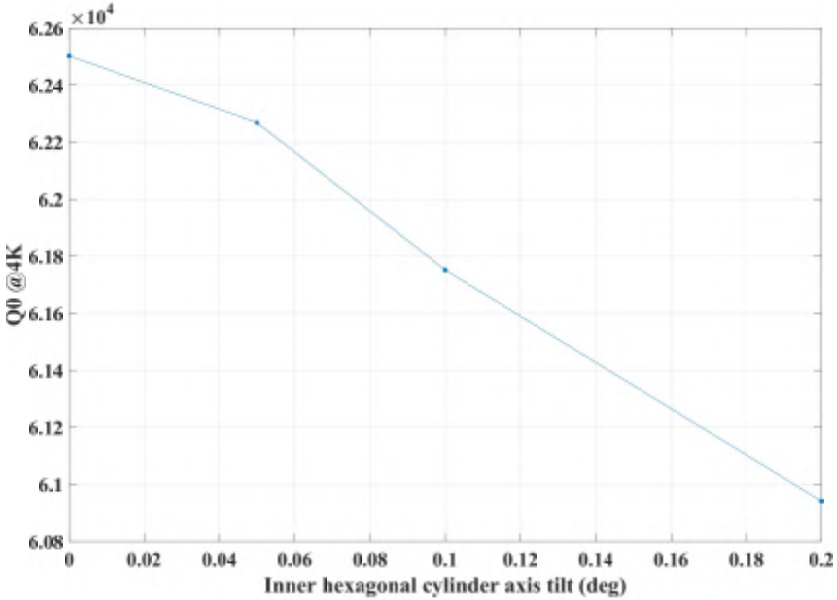

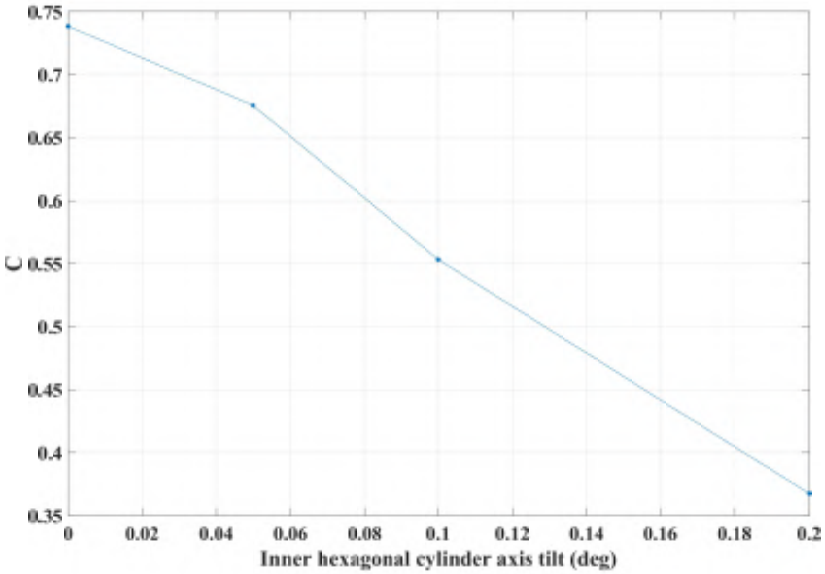

Summary

We successfully employed a large bandwdth, low noise Traveling Wave Parametric Amplifier during an axion search under a 8T magnetic field

90% Confidence Level upper limit on $g_{a\gamma\gamma}$ set in the range 42.8178 - 42.8190 μeV, with peak sensitivity $1.2 \cdot g_{\gamma,KSVZ}$ for the first time inside the axion model band above 10 GHz

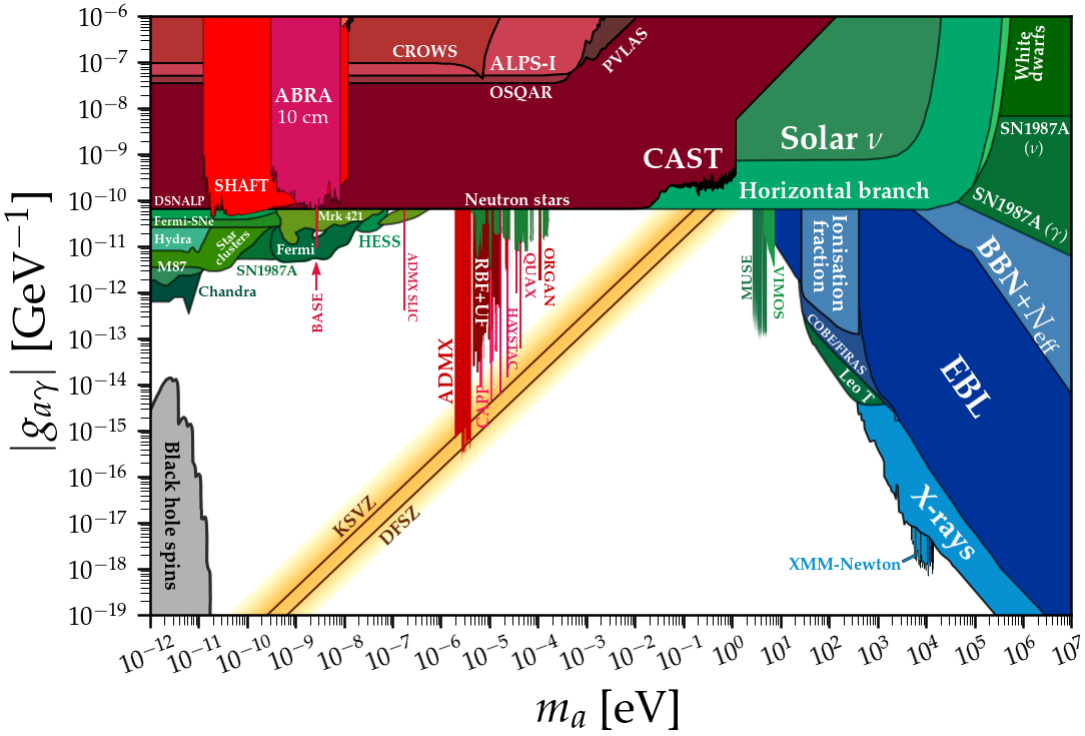

Cavity development proceeds in parallel on dielectric and novel designs:

High V_{eff} dielectric cavity recently tested at cryogenic temperatures showing tuning of 90 MHz @ 10 GHz with close to no mode crossings

Preliminary simulations and tests on high V_{eff} coaxial design suggest technical feasibility

Additional dry dilution fridge installed to allow for parallel development of quantum counter-based setup

Future perspectives

Many substantial upgrades planned:

- Upon noticing the ADC aliasing issue, additional RF filters were installed and we already have verification that the issue has been solved
- A microwave single photon counter with dark count rate below the SQL equivalent PSD will allow to further reduce the system noise temperature; the first prototype has already been tested in Paris by our group in a mock haloscope search
- A Nb3Sn magnet insert (currently in the latter stages of commissioning) will increase the magnetic field to 14 T
- New cavities with $V_{eff} \sim 0.54$ l, $Q_0 \sim 250000$ and $V_{eff} \sim 0.88$ l, $Q_0 \sim 60000$ respectively promise a further improvement in the scan rate
- Upgrades in the instruments control hardware and software toward automatization of the haloscope operation

The detector should then be able to probe the QCD axion parameter space above DFSZ sensitivity and start to operate as a full time observatory

Thank you for the attention!

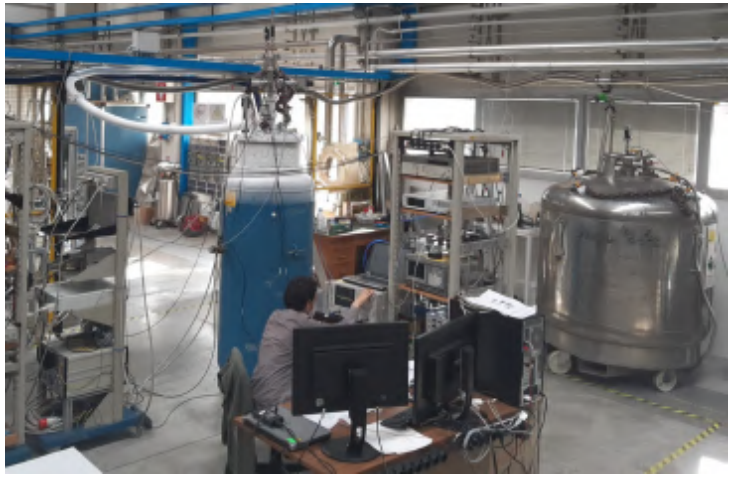

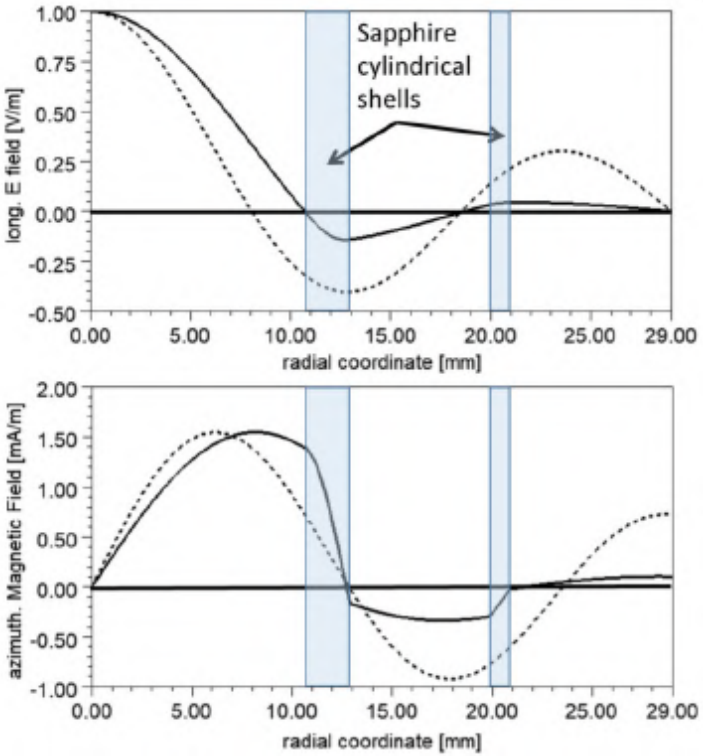

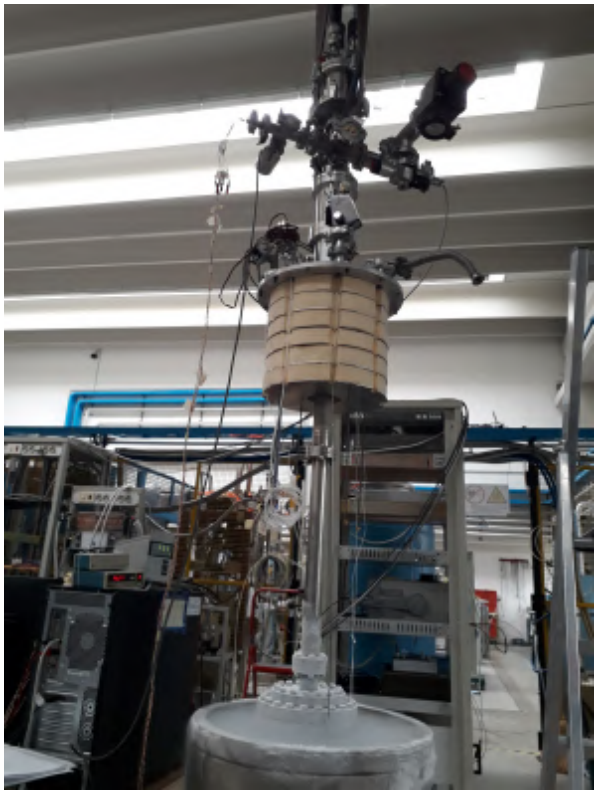

PRELIMINARY experimental results: tuning

- Tunable 420 mm-long aluminium hexagonal cavity mounted on support allowing manual bead pulling in several positions
- Inner surface covered with copper tape to improve Q

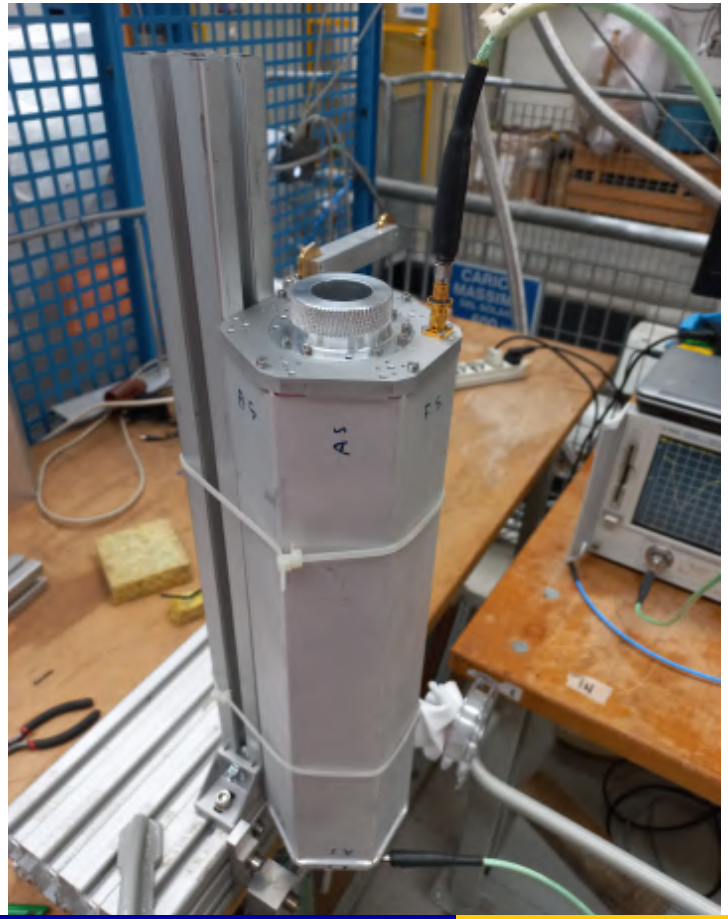

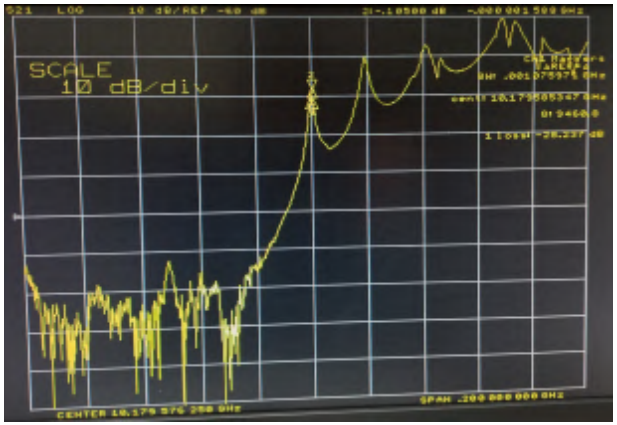

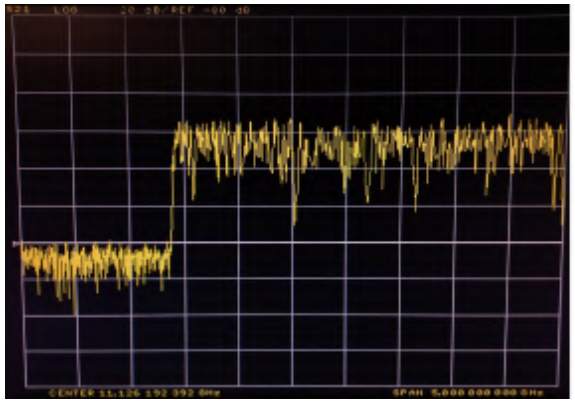

0° tuning

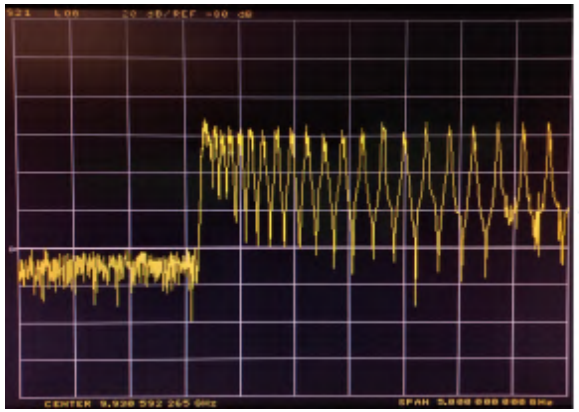

30° tuning

PRELIMINARY experimental results: bead pulling

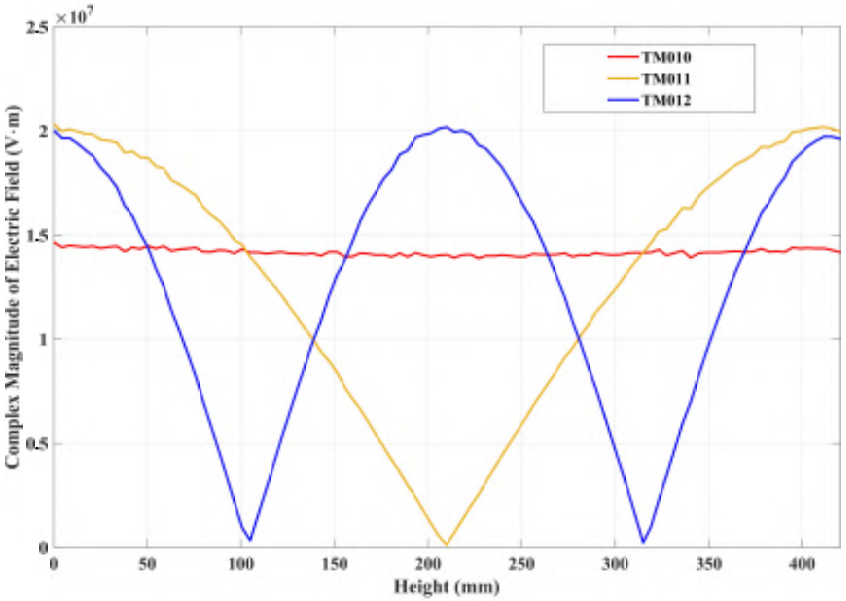

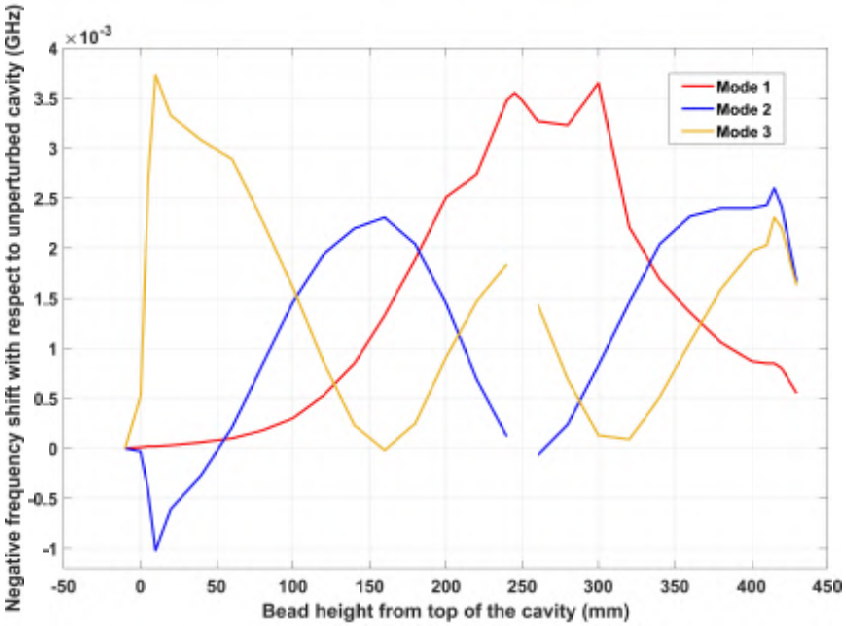

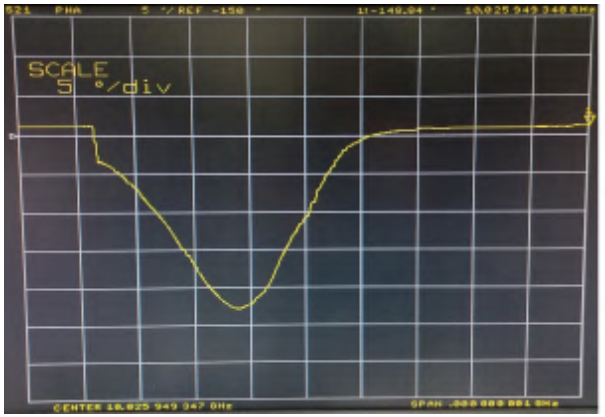

TM010

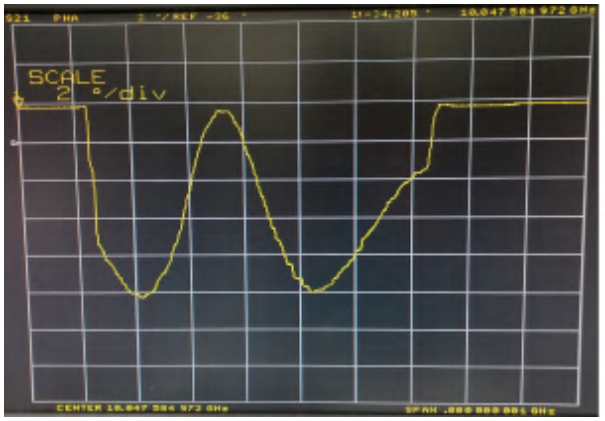

TM011

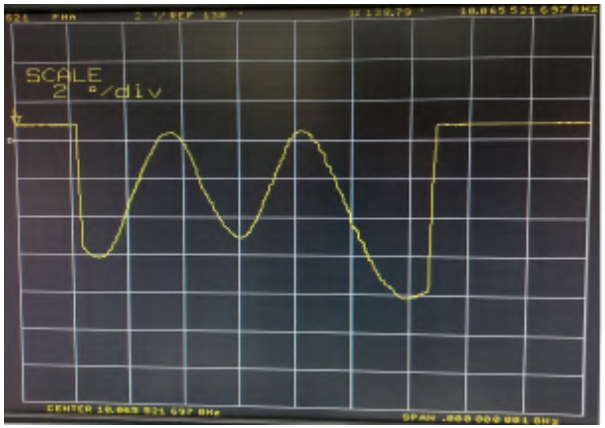

TM012
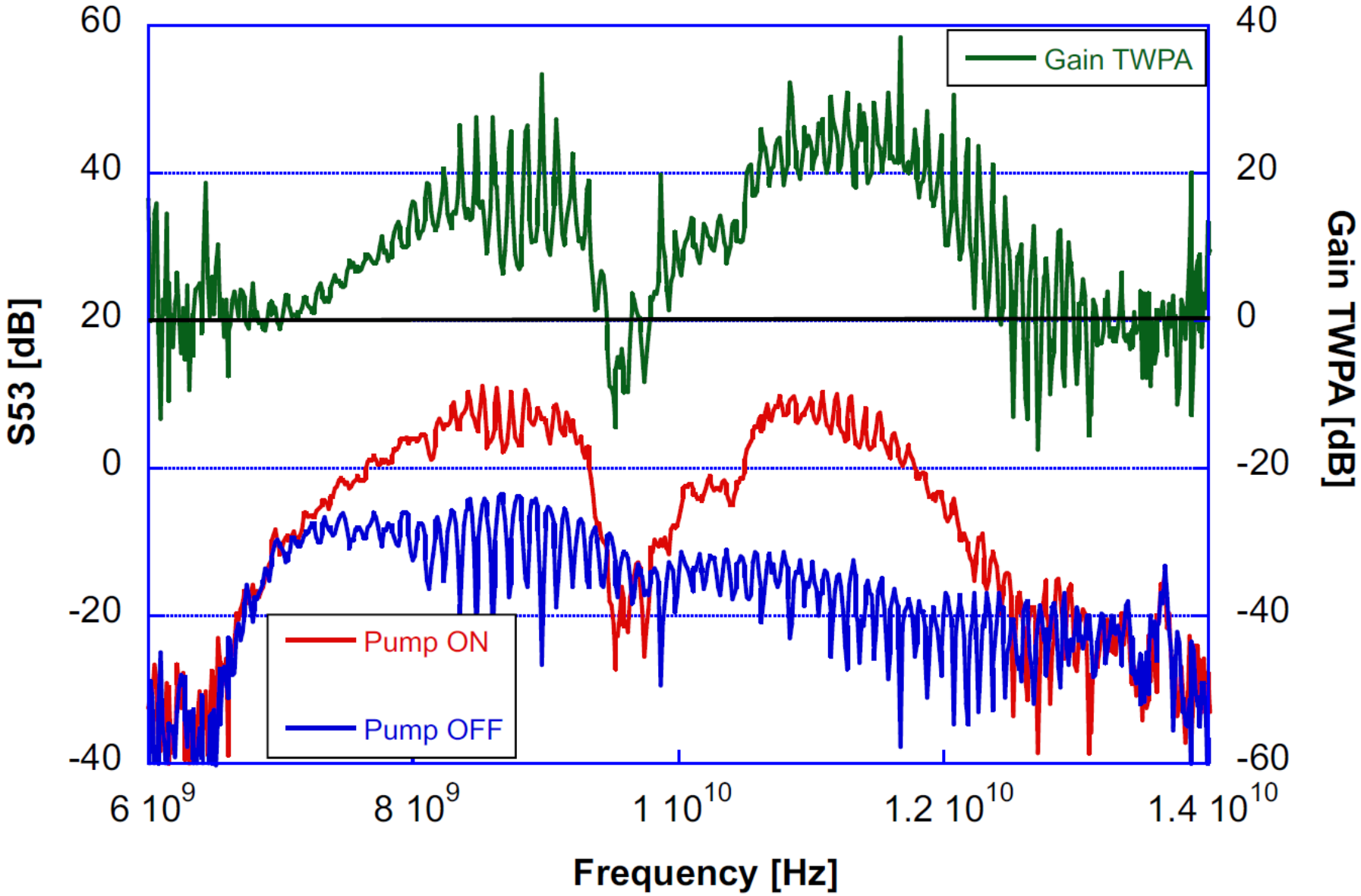
Appendix: TWPA gain and bandwidth